# UNIVERSITÀ DEGLI STUDI DI PADOVA

**Dipartimento di Fisica e Astronomia "Galileo Galilei"**

**Mster's Degree in Physics**

Master's Thesis

# Triple Higgs Production

**Supervisor**

**Prof. Ramona Gröber**

**Student**

**Giancarlo Zilli**

**Anno Accademico 2023/2024**

# Abstract

Multi-Higgs Production allows us to probe the Higgs self-couplings. Due to dominance of the Higgs to top couplings, those processes are dominantly mediated by gluon fusion processes which are at leading order already loop induced.

Triple Higgs production exhibits cross sections of the order of attobarn and is as such beyond the reach of the LHC. Nevertheless, sensitivity studies have been started by experimental collaborations, and the process has also gained interest by the theory community mostly in the context of physics beyond the Standard Model.

Computations of two-loop processes for $2 \rightarrow 3$ kinematics with massive loops are on the forefront of what can be currently done within the field of precision calculations. Triple Higgs production provides a case study to test new analytic or semi-analytic methods to be applied to the computation of the NLO QCD corrections. In this thesis, we calculate the exact LO cross section of Triple Higgs production at the LHC.

Afterwards we apply the transverse momentum expansion technique for the first time to a $2 \rightarrow 3$ process in order to reduce the amount of scale and verify that it correctly reproduces the exact behaviour in its region of validity.

# Contents

# Chapter 1

# Introduction

The discovery of the Higgs boson in 2012 [1, 2] has marked a turning point towards the understanding of the fundamental interactions in nature. The data so far confirms the validity of the Standard Model (SM) of particle physics with high precision.

The SM is a Quantum Field Theory (QFT) based on a Gauge Symmetry Group $SU(3)_C \times SU(2)_L \times U(1)_Y$ [3–5]. The electroweak sector $SU(2)_L \times U(1)_Y$ is broken down to $U(1)_{em}$ by Spontaneous Symmetry Breaking (SSB) of a scalar field: the Higgs field [6, 7].

Thanks to this, fermions and massive gauge bosons, obtain a mass proportional to the Vacuum Expectation Value (VEV) of the Higgs field, without breaking Gauge Invariance.

The Standard Model explains the SSB introducing only one scalar doublet, which is composed of four degrees of freedom, three of which are "eaten up" by the $W^\pm$ and $Z$ bosons to give them masses, and the last one is the physical Higgs boson particle.

Measuring the properties of the Higgs boson is one of the main targets of the LHC. Indeed the Higgs boson was observed in 2012, its mass is known precisely [8], and also its spin and parity are understood [9]. Moreover, some of the Higgs couplings have been measured with remarkable precision [10, 11], i.e. the couplings to the massive vector bosons and the third generation fermion couplings; but its self-couplings have not been experimentally probed yet.

The Higgs self-interactions in the SM are fully determined by the Higgs mass and the VEV. Various beyond-the SM extensions though predict them to differ sizeably from the SM value. So far experimentally they have not been verified yet, e.g. for the trilinear Higgs self-coupling only bounds within $[-1.24, 6.49]$ [11] times its SM value exist. The measurement of the Higgs self-couplings is of utmost importance since their measurement gives access to the Higgs potential – the very origin of electroweak symmetry breaking.

The Higgs self-couplings can be determined experimentally observing double and triple Higgs production. These processes exhibit a direct dependence on the Higgs self-couplings and so they can be used to constrain them and see if there is agreement with the Standard Model predictions.

A lot of effort has gone into the predictions for double-Higgs production coming from the SM and BSM theories also at higher order in the perturbative expansion [12, 13].

The triple Higgs production cross section, instead, is known without approximations only at Leading Order (LO), and, being a gluon fusion initiated process, is expected to have large QCD corrections. While not being valid, those have been estimated in the infinite top mass limit [14] In the first part of this thesis, an analytical result for the triple-Higgs production cross section in the SM at LO is presented.

In the second part of the thesis, an approximation for the pentagon diagrams is discussed. That is, the transverse momentum ($p_t$) expansion, a method used to efficiently approximate other gluon-initiated top-quark loop processes [15–17].

In chapter 2 we give a brief presentation of the Standard Model, focusing especially on the SSB mechanism to fix some of the notation used in the rest of the thesis.

In chapter 3 we focus on the cross section of Triple Higgs Production at the LHC, giving a brief description of the Parton Model and setting the notation for the 2→3 particle phase-space.

In chapter 4 we calculate the complete amplitude for the partonic process.

Finally, in chapter 5, we describe the $p_t$ expansion and we apply it to the LO partonic cross section and check its range of validity.

# Chapter 2

# Theoretical framework

In this section, a brief recap of the Standard Model is presented; in particular, after a comprehensive overview, the focus will be on Spontaneous Symmetry Breaking (SSB) mechanism, to fix the notation used in the rest of the thesis.

## 2.1 Overview of the Standard Model

The Standard Model (SM) of particle physics is a comprehensive theory of electroweak and strong interactions.

The SM could so far predict the interactions among elementary particles with remarkable precision. However, it contains some free parameters that need to be fixed by experiments (26 or 28 depending on the nature of neutrinos). In 2012, ATLAS and CMS announced the discovery of a scalar resonance with a mass around 125 GeV at the LHC [1,2]. So far, this scalar resonance seems compatible with the SM Higgs boson, the last ingredient needed to explain SSB [18].

### 2.1.1 The Gauge group

The SM is a Yang-Mills theory [19] based on the symmetry group:

$$G_{SM} = SU(3)_C \times SU(2)_L \times U(1)_Y. \tag{2.1}$$

The number of generators of $SU(N)$ (corresponding to the number of force carriers) is $N^2 - 1$, so we get 8 gluons from $SU(3)_C$, three gauge bosons from $SU(2)_L$, and one from $U(1)_Y$.

The number of diagonal generators, which corresponds to the fundamental charges, is $N - 1$. Before SSB, we have the color charge, the third component of the isospin charge $T^3$ (known as the weak isocharge), and the weak hypercharge $Y$.

After SSB, the SM symmetry group breaks into:

$$G_{SM}^{SSB} = SU(3)_C \times U(1)_{em}, \tag{2.2}$$

which confirms the fact that gluons and photons remain massless after SSB. The charge related to $U(1)_{em}$ is $Q$, the electric charge in units of $e$ (so for the electron we have $Q_e = -1$) and we get the following relation:

$$Q = T^3 + Y. \tag{2.3}$$

### 2.1.2 The particle content

The particle content of the theory is given by:

- The gauge fields (vector bosons):

$$G_\mu^a, \quad W_\mu^b, \quad B_\mu, \tag{2.4}$$

  that transform respectively in the adjoint of $SU(3)_C$, $SU(2)_L$ and $U(1)_Y$, where $a = 1, ..., 8$ is the color index; $b = 1, 2, 3$ is the weak isospin index. The electroweak gauge fields are recombined with a linear transformation to obtain the physical vector bosons:

$$G_\mu^a, \quad W_\mu^\pm, \quad Z_\mu, \quad A_\mu. \tag{2.5}$$

- The Higgs boson, a doublet under $SU(2)_L$ composed by two complex components, corresponding to 4 real degrees of freedom:

$$\phi = \frac{1}{\sqrt{2}} \begin{pmatrix} \phi_1 + i\phi_2 \\ \phi_3 + i\phi_4 \end{pmatrix} \xrightarrow{SSB} \phi = \frac{1}{\sqrt{2}} \begin{pmatrix} 0 \\ v + H \end{pmatrix}, \tag{2.6}$$

  where $v$ is the vacuum expectation value (VEV) of the Higgs field and $H$ is the new field representing the excitation around the vacuum. The latter expression is chosen in the unitary gauge, where the other three real degrees of freedom are eaten by the massive gauge bosons. The fundamental charges of the Higgs field are:

$$T_3^\phi = \begin{pmatrix} \frac{1}{2} \\ -\frac{1}{2} \end{pmatrix}, \quad Q^\phi = \begin{pmatrix} 1 \\ 0 \end{pmatrix}, \quad Y^\phi = \frac{1}{2}. \tag{2.7}$$

  and it is sterile under $SU(3)_C$.

- Six fermionic doublets under $SU(2)_L$, three quark doublets and three lepton doublets, respectively:

$$Q_L^1 = \begin{pmatrix} u_L \\ d_L \end{pmatrix}, \quad Q_L^2 = \begin{pmatrix} c_L \\ s_L \end{pmatrix}, \quad Q_L^3 = \begin{pmatrix} t_L \\ b_L \end{pmatrix},$$
$$L_L^1 = \begin{pmatrix} \nu_L^e \\ e_L \end{pmatrix}, \quad L_L^2 = \begin{pmatrix} \nu_L^\mu \\ \mu_L \end{pmatrix}, \quad L_L^3 = \begin{pmatrix} \nu_L^\tau \\ \tau_L \end{pmatrix}. \tag{2.8}$$

  Actually we do not need to carry all 6 doublets all the way, we can group them in three generations: the three up-type quarks $u^i = u, c, t$ have the same fundamental charges and differ only in their masses, and so do the down-type quarks $d^i = d, s, b$. The three quark doublets $Q^i$ are formed by an $i$th generation up-type and down-type quark. In the same way we can group the leptons in three doublets $L^i$.

$$Q_L^i = \begin{pmatrix} u_L^i \\ d_L^i \end{pmatrix}, \quad L_L^i = \begin{pmatrix} \nu_L^i \\ e_L^i \end{pmatrix}, \tag{2.9}$$

  where $i = 1, 2, 3$ denotes the generation.
  Both transform under $SU(2)_L$ and $U(1)_Y$, while the quark doublet transforms also under $SU(3)_C$. The fundamental charges are:

$$T_3^Q = \begin{pmatrix} \frac{1}{2} \\ -\frac{1}{2} \end{pmatrix}, \quad Q^Q = \begin{pmatrix} \frac{2}{3} \\ -\frac{1}{3} \end{pmatrix}, \quad Y^Q = \frac{1}{6},$$
$$T_3^L = \begin{pmatrix} \frac{1}{2} \\ -\frac{1}{2} \end{pmatrix}, \quad Q^L = \begin{pmatrix} 0 \\ -1 \end{pmatrix}, \quad Y^L = -\frac{1}{2}. \tag{2.10}$$

- Three (four) fermionic singlets under $SU(2)_L$, the up and down right quarks, the right charged lepton (and the sterile right-handed neutrino):

$$u_R^i, \ d_R^i, \ e_R^i, \ (\nu_R^i). \tag{2.11}$$

The right-handed neutrino has not yet been observed and we will not focus on its peculiarities.

Like before, only the quarks are charged under $SU(3)_C$, all transform under $U(1)_Y$ and are left invariant under $SU(2)_L$ transformations. The fundamental charges are:

$$
\begin{aligned}
T_3^u &= 0, \ \ Q^u = \frac{2}{3}, \ \ Y^u = \frac{2}{3}, \\
T_3^d &= 0, \ \ Q^d = -\frac{1}{3}, \ \ Y^d = -\frac{1}{3}, \\
T_3^e &= 0, \ \ Q^e = -1, \ \ Y^e = -1. \\
T_3^\nu &= 0, \ \ Q^\nu = 0, \ \ Y^\nu = 0.
\end{aligned}
\tag{2.12}
$$

### 2.1.3 The SM Lagrangian

The SM Lagrangian can be written in a short-handed form as:

$$
\begin{aligned}
\mathcal{L}_{SM} =\ & \mathcal{L}_{QCD} - \frac{1}{4} W_{\mu\nu}^a W^{\mu\nu,a} - \frac{1}{4} B_{\mu\nu} B^{\mu\nu} \\
& + (D_\mu \phi)^\dagger (D^\mu \phi) - V(\phi^\dagger \phi) + \sum_f \left[ i\overline{f}\gamma_\mu D^\mu f - (\overline{f} y_f \phi f + h.c.) \right].
\end{aligned}
\tag{2.13}
$$

Looking at Eq. (2.13), the first term is the QCD Lagrangian [20], which contains the gluon field strength as well as terms necessary for the quantisation of non-abelian fields [21] and gauge fixing (which we also do not specify for the electroweak sector). It does not contribute to the spontaneous symmetry-breaking mechanism. The next two terms are the kinetic terms of the electroweak vector bosons, written using the $SU(2)_L$ and $U(1)_Y$ field strength tensors, which are, respectively:

$$W_{\mu\nu}^a = \partial_\mu W_\nu^a - \partial_\nu W_\mu^a + g\epsilon^{abc} W_\mu^b W_\nu^c, \ \ B_{\mu\nu} = \partial_\mu B_\nu - \partial_\nu B_\mu, \tag{2.14}$$

where $W_\mu^a$ transforms in the adjoint of $SU(2)_L$, $a = 1, 2, 3$; and $B_\mu$ transforms in the adjoint of $U(1)_Y$.

The first two terms of the second line of Eq. (2.13) are the Higgs kinetic and potential terms. Finally, the last two terms are, respectively, the kinetic term of the fermions, and the Yukawa term, which will be discussed later, and is shown here only schematically.

The covariant derivative appearing in the Lagrangian acts in the following way:

$$D_\mu = \partial_\mu - ig\frac{\sigma^b}{2} W_\mu^b - ig' Y_\phi B_\mu, \tag{2.15}$$

where $g$ and $g'$ are the electroweak coupling constants and are related to the electric charge $e$ through the relation $e = g\sin\theta_W = g'\cos\theta_W$, where $\theta_W$ is the Weinberg angle and $\sigma^a$ are the Pauli matrices.

## 2.2 Electro-Weak Symmetry Breaking

In order to show how the SSB mechanism gives masses to the Gauge Bosons [22], we need to look at the Higgs sector of the SM Lagrangian:

$$\mathcal{L}^{Higgs} = (D_\mu \phi)^\dagger (D^\mu \phi) - V(\phi^\dagger \phi). \tag{2.16}$$

The Higgs potential is given by

$$V(\phi^\dagger\phi) = \mu^2\phi^\dagger\phi + \lambda(\phi^\dagger\phi)^2, \tag{2.17}$$

where $\lambda > 0$ because the potential has to be bounded from below, and $\mu^2$ can have any real value in general.

The potential has a minimum in $\phi = 0$ if $\mu^2 > 0$, however, another minimum appears if $\mu^2 < 0$ for $\langle\phi\rangle = \sqrt{\frac{-\mu^2}{2\lambda}} = \frac{v}{\sqrt{2}}$, if we define $v^2 = \frac{-\mu^2}{\lambda}$.

This means that once the minimum is no longer in the origin, the vacuum state (the Higgs VEV) is in $v$. Experimentally, the value of $v$ is known with high precision and is around $v \simeq$ 246 GeV.

The Higgs field is a doublet under $SU(2)_L$, so we can write it in its exponential form as:

$$\phi = \frac{1}{\sqrt{2}} \begin{pmatrix} 0 \\ v + H(x) \end{pmatrix} e^{i\frac{\xi^a(x)\sigma^a}{2v}}, \tag{2.18}$$

where $H(x)$ is the excitation of the field around its vacuum state and $\xi^a(x)$ are the Goldstone bosons. We can notice how we still have 4 degrees of freedom since the $SU(2)$ index $a$ runs from 1 to 3.

Now we can apply a gauge transformation to get an easier form of the Higgs field, this arbitrary choice is the "Unitary Gauge":

$$\phi \to \phi' = U\phi = \frac{1}{\sqrt{2}} \begin{pmatrix} 0 \\ v + H(x) \end{pmatrix}, \quad U(x) = e^{-i\frac{\xi^a(x)\sigma^a}{2v}}. \tag{2.19}$$

In this gauge, linear combinations of the other three would-be Goldstone bosons (the $\xi^a(x)$ fields) are said to be "eaten" by the weak gauge bosons. In practice we have rotated away the three Goldstone fields, and they will only appear as the longitudinal polarizations of the $W$ and $Z$ bosons. The vacuum field reads:

$$\langle 0| \phi |0\rangle = \frac{1}{\sqrt{2}} \begin{pmatrix} 0 \\ v \end{pmatrix}. \tag{2.20}$$

Now we can substitute the expression of the Higgs vacuum state in the unitary gauge from Eq. (2.20) in the kinetic Higgs Lagrangian, Eq. (2.16), to get the vector boson masses (substituting from the beginning $Y_\phi = \frac{1}{2}$):

$$\mathcal{L}_{U.G.}^{mass} = (D_\mu\phi)^\dagger(D^\mu\phi) =$$

$$\frac{1}{2}\left[\left(\partial_\mu - ig\frac{\sigma^a}{2}W_\mu^a - ig'\frac{1}{2}B_\mu\right)\begin{pmatrix} 0 \\ v \end{pmatrix}\right]^\dagger\left[\left(\partial_\mu - ig\frac{\sigma^a}{2}W_\mu^a - ig'\frac{1}{2}B_\mu\right)\begin{pmatrix} 0 \\ v \end{pmatrix}\right] =$$

$$\frac{1}{2}v^2\begin{pmatrix} 0 & 1 \end{pmatrix}\begin{pmatrix} \frac{g}{2}W_\mu^3 + \frac{1}{2}g'B_\mu & -i\frac{g}{2}W_\mu^2 + \frac{g}{2}W_\mu^1 \\ i\frac{g}{2}W_\mu^2 + \frac{g}{2}W_\mu^1 & -\frac{g}{2}W_\mu^3 + \frac{1}{2}g'B_\mu \end{pmatrix}^2\begin{pmatrix} 0 \\ 1 \end{pmatrix} = \tag{2.21}$$

$$\frac{g^2v^2}{8}\left(W_\mu^1W^{1\mu} + W_\mu^2W^{2\mu}\right) + \frac{v^2}{4}\left(gW_\mu^3 - g'B_\mu\right)^2.$$

Now we can define $W_\mu^\pm = \frac{1}{\sqrt{2}}(W_\mu^1 \mp W_\mu^2)$

$$\Rightarrow \mathcal{L}_{U.G.}^{mass} = \frac{g^2v^2}{4}W_\mu^+W^{-\mu} + \frac{v^2}{4}\left(gW_\mu^3 - g'B_\mu\right)^2. \tag{2.22}$$

These are the mass terms of three massive gauge bosons. The mass of the $W^\pm$ bosons can already be read from the first term of Eq. (2.22): $m_W^2 = \frac{g^2 v^2}{4}$. Instead, to diagonalize the other masses, we should rotate the other two fields. We then define:

$$\begin{cases} Z_\mu = \cos\theta_W W_\mu^3 - \sin\theta_W B_\mu \\ A_\mu = \sin\theta_W W_\mu^3 + \cos\theta_W B_\mu \end{cases} \Longleftrightarrow \begin{cases} B_\mu = \cos\theta_W A_\mu - \sin\theta_W Z_\mu \\ W_\mu^3 = \sin\theta_W A_\mu + \cos\theta_W Z_\mu \end{cases}, \qquad (2.23)$$

where $\tan\theta_W = \frac{g'}{g}$ is the Weinberg angle and the fields $Z_\mu$ and $A_\mu$ are the physical $Z$ boson and the photon

$$\Rightarrow \mathcal{L}_{U.G.}^{mass} = \frac{g^2 v^2}{4} W_\mu^+ W^{-\mu} + \frac{v^2(g^2 + g'^2)}{2 \cdot 4} Z_\mu Z^\mu, \qquad (2.24)$$

$$\Rightarrow m_W^2 = \frac{g^2 v^2}{4}, \quad m_Z^2 = \frac{v^2(g^2 + g'^2)}{4}, \quad m_\gamma^2 = 0. \qquad (2.25)$$

If we now want to get the interaction terms between the vector bosons and the Higgs boson, we just have to make the substitution $v \to v + H(x)$ in Eq. (2.24):

$$\Rightarrow \mathcal{L}_{U.G.}^{int.} = \left(1 + \frac{H}{v}\right)^2 m_W^2 W_\mu^+ W^{-\mu} + \frac{1}{2}\left(1 + \frac{H}{v}\right)^2 m_Z^2 Z_\mu Z^\mu, \qquad (2.26)$$

from which we can directly extract the following Feynman rules, remembering also the combinatorial factors:



## 2.3 Fermionic sector

The fermionic sector is the sum of the last two terms of Eq. (2.13). We now decompose the generic fermionic field $f$, introducing the chirality projectors $P_{L,R}$:

$$f_L = P_L f, \quad f_R = P_R f, \quad P_{L,R} = \frac{\mathbb{1} \mp \gamma_5}{2}, \quad P_R + P_L = \mathbb{1}, \qquad (2.27)$$

$$\Rightarrow P_{L,R}^2 = P_{L,R}, \quad P_L P_R = P_R P_L = 0, \quad f = f_L + f_R, \qquad (2.28)$$

where $f_L = u_L^i, d_L^i, e_L^i, \nu_L^i$ and $f_R = u_R^i, d_R^i, e_R^i$, $i = 1, 2, 3$.

The covariant derivative contains the kinetic term of each fermion and its gauge interactions, while the Yukawa term is responsible for the fermion masses and interactions with the Higgs

boson.

Since quarks have a color charge, we add the interaction with the gluon in the covariant derivative, that acts on the components of the fermion fields as:

$$D_\mu = \partial_\mu - ig_s \frac{\lambda^a}{2} G_\mu^a - ig \frac{\sigma^b}{2} W_\mu^b - ig' Y_\phi B_\mu, \tag{2.29}$$

where $g_s$ is the strong coupling constant, $G^a$ are the eight gluons and $\lambda^a$ are the Gell-Mann matrices: the generators of $SU(3)$ in the fundamental representation.

We rewrite the fermionic sector in the Unitary Gauge, expanding the covariant derivative:

$$\mathcal{L}_F^{U.G.} = \sum_f (\overline{f}_L i \slashed{\partial} f_L + \overline{f}_R i \slashed{\partial} f_R) - \frac{g}{\sqrt{2}}(W_\mu^- J^{+\mu} + W_\mu^+ J^{-\mu})$$
$$- \frac{g}{\cos\theta_W} Z_\mu J_Z^\mu - e A_\mu J_{em}^\mu - g_s G_\mu^a J_S^{a\mu} + \mathcal{L}_Y. \tag{2.30}$$

The index $f$ runs over all the fermionic fields: $f = u, d, c, s, b, t, e, \mu, \tau, \nu_e, \nu_\mu, \nu_\tau$. We have respectively:

- The kinetic terms for the fermions $\sum_f (\overline{f}_L i \slashed{\partial} f_L + \overline{f}_R i \slashed{\partial} f_R)$;

- the electromagnetic current $e A_\mu J_{em}^\mu$, where:

$$J_{em}^\mu = \sum_f Q_f (\overline{f}_L \gamma^\mu f_L + \overline{f}_R \gamma^\mu f_R); \tag{2.31}$$

- the strong current $g_s G_\mu^a J_S^{a\mu}$, where

$$J_S^{a\mu} = \sum_q (\overline{q}_L^i \gamma^\mu T_{ij}^a q_L^j + \overline{q}_R^i \gamma^\mu T_{ij}^a q_R^j), \tag{2.32}$$

where $T_{ij}^a = \frac{\lambda_{ij}^a}{2}$ are the $SU(3)_C$ generators in the fundamental representation, $i,j$ are color indexes and $q$ runs over all the 6 quarks.

- the weak charged current $\frac{g}{\sqrt{2}}(W_\mu^- J^{+\mu} + W_\mu^+ J^{-\mu})$, where

$$J_\mu^- = \sum_{i=1}^3 (\overline{u^i}_L \gamma_\mu d_L^i + \overline{\nu}_L^i \gamma_\mu e_L^i), \quad J_\mu^+ = (J_\mu^-)^\dagger; \tag{2.33}$$

- The weak neutral current $\frac{g}{\cos\theta_W} Z_\mu J_Z^\mu$, where:

$$J_\mu^Z = J_\mu^{3L} - \sin^2\theta_W J_\mu^{em} = \sum_f \left[ \overline{f}_L \gamma_\mu T_3 f_L - \sin^2\theta_W Q_f (\overline{f}_L \gamma^\mu f_L + \overline{f}_R \gamma^\mu f_R) \right]. \tag{2.34}$$

It is crucial to stress that all the kinetic terms and the gauge interactions couple fermions with the same chirality, so all those terms will be gauge invariant.

The problem arises if we try to write a canonical Dirac mass term for the fermions, i.e the up quark, $m\overline{u}u$ because it would violate gauge invariance. We decompose it along the chiral projectors:

$$m\overline{u}u = m(\overline{u}_L + \overline{u}_R)(u_L + u_R) = m(\overline{u}_L u_R + \overline{u}_R u_L). \tag{2.35}$$

However, right- and left-handed fermionic fields are in different representations of the group $SU(2)_L$, (respectively the trivial representation and the fundamental representation), therefore

they transform differently under $SU(2)_L$ and that is the reason why such a term would violate gauge invariance.

In order to avoid such a "catastrophe", we rely again on SSB and write a Yukawa-type interaction:

$$\mathcal{L}_Y = -\overline{Q}_L \phi y_d d_R - \overline{Q}_L \tilde{\phi} y_u u_R - \overline{L}_L \phi y_e e_R - \overline{L}_L \tilde{\phi} y_\nu \nu_R + h.c. \tag{2.36}$$

where $\tilde{\phi} = i\sigma_2 \phi^*$.

It is easy to show that this Lagrangian is gauge invariant since the Higgs field transforms in the fundamental representation of $SU(2)_L$.

In the unitary gauge we get:

$$\phi = \frac{1}{\sqrt{2}} \begin{pmatrix} 0 \\ v + H(x) \end{pmatrix}, \quad \tilde{\phi} = \frac{1}{\sqrt{2}} \begin{pmatrix} v + H(x) \\ 0 \end{pmatrix}. \tag{2.37}$$

Then the Yukawa Lagrangian becomes:

$$\mathcal{L}_Y = -\left(\frac{v + H(x)}{\sqrt{2}}\right) \left(\bar{d}_L y_d d_R + \bar{u}_L y_u u_R + \bar{e}_L y_e e_R + \bar{\nu}_L y_\nu \nu_R + h.c.\right). \tag{2.38}$$

and we can easily read the fermion masses $m_f = \frac{y_f v}{\sqrt{2}}$ and the Feynman rule for the interaction between fermions and the Higgs boson from Eq. (2.38):



$$= -\frac{i}{\sqrt{2}} y_f.$$

## 2.4 Higgs sector

Now we can also find the Feynman rules for Higgs self-interactions by looking at the Higgs potential in Eq. (2.17). Being still in the unitary gauge, we find:

$$\mathcal{L}^H = \frac{\lambda v^2}{2}\left(v^2 + 2vH + H^2\right) - \frac{\lambda}{4}\left(v^4 + 4v^2 H^2 + H^4 + 4v^3 H + 4vH^3 + 2v^2 H^2\right), \tag{2.39}$$

$$\Rightarrow \mathcal{L}^H = -\lambda v^2 H^2 - \lambda v H^3 - \frac{\lambda}{4} H^4, \tag{2.40}$$

from which we can easily read the Higgs mass ($m_H^2 = 2\lambda v^2$) and the Feynman rules for its self interactions:



$$= -i\lambda v 3!$$

$$= -i\frac{\lambda}{4} 4!$$

In the SM, the strength of the Higgs self-interactions, given by the adimensional parameter $\lambda$, is fixed in terms of the Higgs boson mass:

$$\lambda = \frac{m_H^2}{2v^2}, \tag{2.41}$$

that has been determined experimentally. This means that within the SM the Higgs self-couplings are determined. It is though anyways crucial to measure them, as this would provide the ultimate test of electroweak symmetry breaking by confirming the form of the Higgs potential.

In Tab. 2.1 the degrees of freedom and the mass spectrum before and after SSB are recapped. As can be inferred from the table, clearly the degrees of freedom remain the same even though assigned to different fields.

| $\mu^2 < 0$ | | | $\mu^2 > 0$ | | |
|---|---|---|---|---|---|
| Particle | mass$^2$ | d.o.f | Particle | mass$^2$ | d.o.f |
| $W_\mu^\pm$ | $\frac{g^2 v^2}{4}$ | $2 \times 3 = 6$ | $W_\mu^a$ | $0$ | $3 \times 2 = 6$ |
| $Z_\mu$ | $\frac{(g^2 + g'^2) v^2}{4}$ | $1 \times 3 = 3$ | $B_\mu$ | $0$ | $1 \times 2 = 2$ |
| $A_\mu$ | $0$ | $1 \times 2 = 2$ | $\phi$ | $\mu^2$ | $4 \times 1 = 4$ |
| $H$ | $2\lambda v^2$ | $1 \times 1 = 1$ | | | |
| | | TOT=12 | | | TOT=12 |

Table 2.1: Gauge Bosons and Higgs mass spectrum before and after SSB.

# Chapter 3

# Cross Section

In this chapter we will present the structure of the triple-Higgs production cross section at the LHC. The first section will contain a brief description of the parton model, the second one will be about the phasespace of a three-particle process, and the third one about the numerical method used to do the multidimensional integral.

## 3.1 The Parton Model

The LHC or any hadron collider requires to know the elementary particle content of the hadrons involved in the considered particle reaction.
We can though still use perturbation theory to calculate cross sections of processes at hadron colliders if we start from three principles:

- the asymptotic freedom of Quantum Chromodynamics (QCD) [23]

- the validity of the parton model [24]

- the property of factorization in hadronic cross sections

It is possible to understand that QCD is indeed an asymptotic free theory by calculating the running of the strong coupling constant $g_s$ with the renormalization scale already at one loop. Contrary to the electric charge, which grows with the energy, the strong coupling constant becomes smaller and smaller as the energy grows, with a pole for energies $\mu \simeq \Lambda_{QCD}$ that separates perturbative QCD from non-perturbative effects with the following profile:

$$g_s(\mu) \sim \ln^{-1}\left(\frac{\mu}{\Lambda_{QCD}}\right). \tag{3.1}$$

This means that the strong-coupling constant can be used to perform a perturbative expansion of the amplitudes only for energies larger than the QCD pole implying that the hard scattering processes of quarks and gluons can be computed within perturbation theory. However, the long-distance effects due to low-energy QCD of the strong interaction are not calculable with the usual description of the Feynman diagrams. These effects include the interactions between quarks and gluons inside the protons accelerated at the LHC.
To have a quantitative description of what happens in the scattering of high energy hadrons, we assume the parton model is valid.
We also use the property of factorization in hadronic cross sections: we assume that low- and high-energy QCD effects can be treated independently, so we can factorize them in the cross section. These three assumptions hold with a very high level of precision, and thanks to

them, we can do precision calculations for hadron scatterings even if we have not yet explained hadronization at low-energies.

Let's then use these assumptions to write a formula to calculate the cross section $\sigma$ of scatterings at the LHC:

$$\sigma = \sum_{a,b} \int dx_1 dx_2 \Theta(x_1 x_2 - \tau_1) f_a(x_1, \mu_F) f_b(x_2, \mu_F) \hat{\sigma}_{ab}(x_1, x_2, Q, \mu_F) + \mathcal{O}\left(\frac{\Lambda_{QCD}}{Q}\right), \quad (3.2)$$

where $\sigma_{ab}$ is the so-called *partonic* cross section of the hard scattering of partons $a$ and $b$. As one can see from Eq. (3.2), the partonic cross section is convoluted with the Parton Distribution Functions (PDFs) $f_a$ and $f_b$, the probability that the partons $a$ and $b$ carry a fraction of the momentum $x_1$ and $x_2$ of the incoming protons at factorization scale $\mu_f$. The latter is the arbitrary energy scale that separates long-distance to short-distance QCD effects. The profile of the PDFs is known only numerically from a fit to experimental data and in this thesis is taken from the public database LHAPDF [25] (set `NNPDF40-lo-as-01180` [26]). Finally, $Q$ is the characteristic energy scale of the partonic process, $\Theta$ is the Heaviside theta function and $\tau_1$ is a constant that reflects a kinematical constraint, in our case the center of mass (CoM) energy of the partonic process needs to be large enough to produce three on-shell Higgs bosons (more on this later).

For the process studied in this thesis, the only relevant contribution to the total cross section is the one coming from Gluon Fusion (GF), so $a = b = g$ in Eq. (3.2).

## 3.2 Partonic cross section

In this section, we will analyze the partonic cross section, and in particular the three-particle phasespace [27]. First of all, let's specify the kinematic variables.

The four-momenta of the incoming protons will be denoted with the capital letter, so we have $P_1$ and $P_2$ for the first and second proton respectively. We denote by $s = (P_1 + P_2)^2$ the invariant mass of the process, which is also the squared (CoM) energy of the two incoming protons, which we assume to be $\sqrt{s} = E_{CM} = 14$ TeV.

We label the partonic process with the following momenta:

$$g_\mu^a(p_1) + g_\nu^b(p_2) \to H(p_3) + H(p_4) + H(p_5), \quad (3.3)$$

where $a, b$ are the color indexes for the gluons and $\mu, \nu$ are Lorentz indexes. The gluons are taken incoming, whereas the Higgs are taken outgoing. This means that the momenta conservation reads:

$$p_1 + p_2 = p_3 + p_4 + p_5. \quad (3.4)$$

The particles are on-shell, so:

$$p_3^2 = p_4^2 = p_5^2 = m_H^2, \qquad p_1^2 = p_2^2 = 0. \quad (3.5)$$

As explained in the previous section, the momenta of the gluons can be written as:

$$p_1 = x_1 P_1, \qquad p_2 = x_2 P_2. \quad (3.6)$$

From now on, variables with a hat will be understood as partonic variables. Therefore, the partonic COM energy is related to the total one with:

$$\hat{s} = \tau s, \quad \tau = x_1 x_2. \quad (3.7)$$

Being a $2 \to 3$ process, there is not a convention on generalizing the Mandelstam variables. However, it is clear that the amplitude will depend on five independent kinematical variables (other than the particle masses). In this work, we use the following:

$$\hat{s} = (p_1 + p_2)^2, \quad \hat{s}_1 = (p_3 + p_4)^2, \quad \hat{s}_2 = (p_4 + p_5)^2,$$
$$\hat{t}_1 = 2p_1 \cdot p_3 = m_H^2 - (p_1 - p_3)^2, \quad \hat{t}_2 = 2p_2 \cdot p_4 = m_H^2 - (p_2 - p_4)^2. \tag{3.8}$$

The only other energy scale that will enter the amplitude is the top-quark mass $m_t$, which will come out of the fermionic loops.

We also introduce two other variables that we will use later, useful for getting more compact expressions even if they are not independent:

$$\hat{u}_1 = 2p_2 \cdot p_3 = m_H^2 - (p_2 - p_3)^2 = \hat{s} - \hat{t}_1 - \hat{s}_2 + m_H^2,$$
$$\hat{u}_2 = 2p_1 \cdot p_4 = m_H^2 - (p_1 - p_4)^2 = \hat{s}_1 + \hat{s}_2 - \hat{t}_2 - 2m_H^2. \tag{3.9}$$

The partonic cross section is calculated in the CoM frame of the gluons, for which we have a well-known formula:

$$\hat{\sigma}(\hat{s}) = \frac{1}{2E_1} \frac{1}{2E_2} \frac{1}{|\overline{v_1} - \overline{v_2}|} \int d\Pi_3 |\overline{\mathcal{A}}|^2, \tag{3.10}$$

where the energies of the gluons in this frame are $E_1 = E_2 = \hat{E}_{CM}/2$, $\overline{v}_i = \overline{p}_i/E_i$ are the 3-velocities of the gluons ($\overline{p}_i$ are the 3-momenta), $|\overline{\mathcal{A}}|^2$ is the unpolarized squared amplitude of the process, and $d\Pi_3(p_1, p_2, p_3, p_4, p_5)$ is the Lorentz-invariant 3-particle phasespace, that generalizes for $N$ particles this way:

$$d\Pi_N = (2\pi)^4 \delta^{(4)} \left( \sum_{i=1,2} p_i - \sum_{f=3,...,N} p_f \right) \prod_{\text{final states } f} \frac{d^3 \overline{p}_f}{(2\pi)^3 2E_f}, \tag{3.11}$$

where the Dirac Delta represents the conservation of the 4-momentum. This expression for the phasespace can be simplified using a mathematical trick.

The $2 \to N$ process can be in fact decomposed into a cascade of $N-1$ $2 \to 2$ scatterings [28], like depicted in Fig. (3.1):



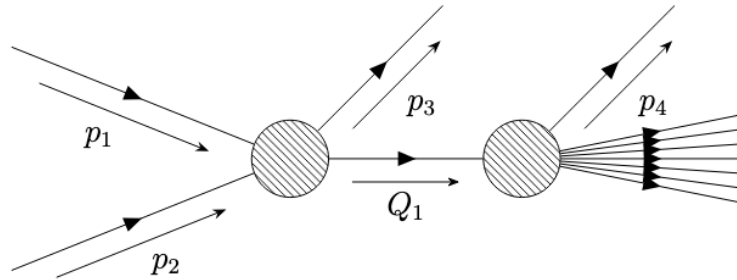Figure 3.1: Decomposition of a $2 \to N$ process into a cascade of $2 \to 2$ subprocesses to easy the computation of the phasespace.

So, the $N$-particle phasespace factor in Eq. (3.11) can be seen as a product of $N-1$ terms, each one being an intermediate 2-particle phasespace factor.

$$d\Pi_N(p; p_3..., p_N) = \frac{dQ_1^2}{2\pi} d\Pi_2(p; Q_1, p_3) d\Pi_{N-1}(Q_1; p_4, ..., p_N), \tag{3.12}$$

where $p_i$, $i = 1, ..., N$ are the momenta of the particles involved, $p = p_1 + p_2$ is the momentum of the two initial particles and:

$$Q_1 = p_4 + ... + p_N \Rightarrow Q_1^2 = Q_{10}^2 - \overline{Q}_1^2 \Rightarrow dQ_1^2 = 2Q_{10}dQ_{10}. \tag{3.13}$$

It is easy to show that Eq. (3.12) and Eq. (3.11) represent the same quantity, we start by expanding the phasespace factors and the first differential from Eq. (3.12) :

$$d\Pi_N = \frac{Q_{10}dQ_{10}}{2\pi} \frac{d^3\overline{Q}_1}{(2\pi)^3 2Q_{10}} \frac{d^3\overline{p}_3}{(2\pi)^3 2E_3} (2\pi)^4 \delta^{(4)}(p-Q_1-p_3) \prod_{j=4}^{N} \frac{d^3\overline{p}_j}{(2\pi)^3 2E_j} (2\pi)^4 \delta^{(4)}(Q_1-p_4-...-p_N). \tag{3.14}$$

Now we rearrange Eq. (3.14), noticing that we can rewrite the product of the first two differentials as $d^4Q_1$

$$d\Pi_N = d^4Q_1 \delta^{(4)}(p - Q_1 - p_3) \prod_{j=3}^{N} \frac{d^3\overline{p}_j}{(2\pi)^3 2E_j} (2\pi)^4 \delta^{(4)}(Q_1 - p_4 - ... - p_N). \tag{3.15}$$

Now we solve for the first Dirac Delta getting rid of the $d^4Q_1$ integration obtaining the condition $Q_1 = p - p_3$, and finding Eq. (3.11), hence we demonstrated that indeed the $N$ phase space can computed as in Eq. (3.12).

Returning to the 2→3 process, we can then write the 3-particle phasespace as:

$$d\Pi_3(p_1, p_2; p_3, p_4, p_5) = \frac{d\hat{s}_2}{2\pi} d\Pi_2(p; p_3, p_4 + p_5) d\Pi_2(p_4 + p_5; p_4, p_5), \tag{3.16}$$

where the expressions for the 2-particle phasespace is trivial and specifies to our cases as:

$$d\Pi_2(p; p_3, p_4 + p_5) = \frac{d\hat{t}_1}{8\pi\hat{s}}, \tag{3.17}$$

$$d\Pi_2(p_4 + p_5; p_4, p_5) = \frac{d\hat{t}_2 d\varphi}{16\pi^2(\hat{s}_2 + \hat{t}_1 - m_H^2)}, \tag{3.18}$$

where $\varphi$ is the azimuthal angle relative to the 4th Higgs in spherical coordinates. In our calculation, we actually adopt a change of variable $\varphi \rightarrow \hat{s}_1$. It will bring a factor $J_1$ in the integration of the phase space coming from the Jacobian of the transformation, and the new limits of integration will be denoted by $\hat{s}_{1\pm}$ (the full expressions can be found in the Appendix in Eq. (A.1)).

The other limits of integration are the following:

$$\begin{cases} \hat{s}_{2-} = 4m_H^2 \leq \hat{s}_2 \leq (\sqrt{\hat{s}} - m_H)^2 = \hat{s}_{2+} \\ 0 \leq \varphi \leq 2\pi \\ \hat{t}_{i-} \leq \hat{t}_i \leq \hat{t}_{i+}, \quad i = 1, 2 \end{cases}, \tag{3.19}$$

$$\hat{t}_{1\pm} = \frac{1}{2}(\hat{s} + m_H^2 - \hat{s}_2 \pm \sqrt{\lambda_1}), \quad \hat{t}_{2\pm} = \frac{1}{2}\frac{\hat{s}_2 + \hat{t}_1 - m_H^2}{\hat{s}_2}(\hat{s}_2 \pm \sqrt{\lambda_2}), \tag{3.20}$$

where the $\lambda_i$ are functions of the other energy scales:

$$\lambda_1 = (\hat{s} + m_H^2 - \hat{s}_2)^2 - 4m_H^2\hat{s}, \quad \lambda_2 = \hat{s}_2^2 - 4m_H^2\hat{s}_2. \tag{3.21}$$

So the partonic cross section is written as:

$$\hat{\sigma} = \frac{1}{2E_1}\frac{1}{2E_2}\frac{1}{|\overline{v_1} - \overline{v_2}|} \int_{\hat{s}_{2-}}^{\hat{s}_{2+}} \frac{d\hat{s}_2}{2\pi} \int_{\hat{t}_{1-}}^{\hat{t}_{1+}} \frac{d\hat{t}_1}{8\pi\hat{s}} \int_{\hat{t}_{2-}}^{\hat{t}_{2+}} \frac{d\hat{t}_2}{16\pi^2(\hat{s}_2 + \hat{t}_1 - m_H^2)} \int_{\hat{s}_{1-}}^{\hat{s}_{1+}} d\hat{s}_1 J_1 |\overline{\mathcal{A}}|^2. \tag{3.22}$$

## 3.3    Multidimensional integration

In this section there will be a brief description of the method used to integrate the total cross section.

Looking at Eq. (3.11), it seems that the partonic cross section is the result of a $3N$-dimensional integration, where $N$ is the number of particles in the final state ($N = 3$ here). However, the conservation of the 4-momentum gives 4 independent conditions, so we only have to integrate $3N - 4 = 5$ variables. We also have to consider that the unpolarized amplitude will not depend on the orientation of the reference frame, so one azimuthal angle will be a dummy variable, giving only a $(2\pi)$ factor, already included in Eq. (3.22). So, the number of variables to integrate is 4.

We also have to consider the integration of $x_1$ and $x_2$ to obtain the total cross section at the LHC, so we have to deal with a non-trivial 6-dimension integral.

Given the multi-dimensionality of the integration as well as the fact that the PDFs are numerical, the right tool is to use a Monte Carlo integration in order to obtain the cross section. For this purpose, we wrote a FORTRAN program (B.1), using a Monte Carlo integration routine known as VEGAS [29], using the implementation of the CUBA library [30]. The integration of the phase-space was also checked numerically using RAMBO [31], a Montecarlo event generator algorithm for phase-space distributions

Monte Carlo integration involves the use of random numbers within the interval $[0, 1]^N$ for an $N$-dimensional integral. In essence, Monte Carlo integration works by evaluating the integrand at numerous random points generated by a random number generator. The value of the integral is then approximated by averaging the values of the integrand at these random points. This approach is particularly advantageous for handling multidimensional integrals, as it tends to be significantly faster than other traditional integration methods.

However, the VEGAS routine represents a refined version of the Monte Carlo integration technique. To improve the accuracy of the integral, VEGAS employs a method known as importance sampling. Unlike basic Monte Carlo integration, where random numbers are uniformly distributed across the entire integration domain, importance sampling focuses on generating more random numbers in regions where the integrand makes the most significant contributions. This is achieved by constructing a probability distribution that closely models the integrand itself. VEGAS accomplishes this by dividing the integration space into a rectangular grid, performing the integration within each subregion, and iteratively refining the grid based on where the integral is most heavily concentrated. This iterative adjustment allows VEGAS to focus on the regions of greatest importance, thus increasing the precision of the integration over successive iterations.

It is worth noting that VEGAS is specifically designed to evaluate integrals within the intervals $[0, 1]^N$. Therefore, if the integral in question has limits outside this range, it must first undergo a substitution of the integration variable that redefines the limits to fall within the said hypercube.

It is particularly beneficial to perform this substitution in a manner that closely mimics the structure of the integrand. When this substitution is done effectively, it facilitates the VEGAS routine's ability to identify the most crucial regions of the integration space. Consequently, this leads to a more rapid convergence of the numerical evaluation of the integral.

In principle, the integration of the PDFs is already done in the right dominium (being $x_1$ and $x_2$ fractions of the protons momenta, they are already in the range $r_i \in [0, 1]$).The hadronic cross section from Eq. (3.2) is:

$$\sigma = \int_0^1 \mathrm{d}x_1 \int_0^1 \mathrm{d}x_2 \Theta(x_1 x_2 - \tau_1) f_1(x_1, \mu_F) f_2(x_2, \mu_F) \hat{\sigma}, \qquad (3.23)$$

where $f_1$ and $f_2$ are the PDFs relative to the two gluons, $\hat{\sigma}$ is the partonic cross section and $\tau_1 = \frac{(3m_H)^2}{\hat{s}}$ is the normalized energy threshold for the process that is added to account for the fact that the production of three on-shell Higgs bosons requires a minimum partonic CoM energy ($\sqrt{\hat{s}} \geq 3\,m_H$). Hence, not all values of $x_1$ and $x_2$ are allowed. Therefore we make the substitution:

$$\tau = x_1 x_2, \quad x = x_1 \Rightarrow \mathrm{d}x_1 \mathrm{d}x_2 = \frac{1}{x_1}\mathrm{d}\tau \mathrm{d}x, \tag{3.24}$$

The limits of integration of the new variables, considering also the role of the Heaviside theta function are now the following:

$$\tau_1 \leq \tau \leq 1, \quad \tau \leq x \leq 1. \tag{3.25}$$

So we obtain:

$$\sigma = \int_{\tau_1}^1 \mathrm{d}\tau \int_\tau^1 \frac{\mathrm{d}x}{x} f_1(x, \mu_F) f_2(\tau/x, \mu_F)\hat{\sigma}. \tag{3.26}$$

Now we adapt the integral to VEGAS by making yet another change of variables:

$$\tau = \tau_1^{r_1}, \quad x = \tau^{r_2} \Rightarrow \mathrm{d}\tau \mathrm{d}x = x\,\tau \ln(\tau)\ln(\tau_1)\mathrm{d}r_1 \mathrm{d}r_2. \tag{3.27}$$

$$\Rightarrow \sigma = \int_0^1 \mathrm{d}r_1 \int_0^1 \mathrm{d}r_2\, \tau \ln(\tau)\ln(\tau_1) f_1(x, \mu_F) f_2(\tau/x, \mu_F)\hat{\sigma}. \tag{3.28}$$

Being a numerical integration, we can safely keep $x$ and $\tau$ instead of writing their dependence on $r_1$ and $r_2$, which are the random numbers given by VEGAS and are indeed in the right range.

The last thing to notice is that the PDF from LHAPDF is not directly $f(x)$, but is $xf(x)$, namely the momentum density. To take this into account, we simply need to make the substitution $f(x) \rightarrow f(x)/x$. This yields

$$(f_1(x, \mu_f) f_2(\tau/x, \mu_f)) \rightarrow (f_1(x, \mu_f) f_2(\tau/x, \mu_f))/\tau. \tag{3.29}$$

At the end we get:

$$\sigma = \int_0^1 \mathrm{d}r_1 \int_0^1 \mathrm{d}r_2 \ln(\tau)\ln(\tau_1) f_1(x, \mu_F) f_2(\tau/x, \mu_F)\hat{\sigma}. \tag{3.30}$$

The partonic cross section is written as Eq. (3.22):

$$\hat{\sigma} = \frac{1}{2E_1}\frac{1}{2E_2}\frac{1}{|\overline{v_1} - \overline{v_2}|}\int \mathrm{d}\Pi_3 |\overline{\mathcal{A}}|^2 =$$
$$\frac{1}{2E_1}\frac{1}{2E_2}\frac{1}{|\overline{v_1} - \overline{v_2}|}\int_{\hat{s}_{2-}}^{\hat{s}_{2+}}\frac{\mathrm{d}\hat{s}_2}{2\pi}\int_{\hat{t}_{1-}}^{\hat{t}_{1+}}\frac{\mathrm{d}\hat{t}_1}{8\pi\hat{s}}\int_{\hat{t}_{2-}}^{\hat{t}_{2+}}\frac{\mathrm{d}\hat{t}_2}{16\pi^2(\hat{s}_2 + \hat{t}_1 - m_H^2)}\int_{\hat{s}_{1-}}^{\hat{s}_{1+}}\mathrm{d}\hat{s}_1 J_1 |\overline{\mathcal{A}}|^2. \tag{3.31}$$

To correctly adapt it to VEGAS, we make the same change of variable to all the 4 partonic integrations. If $\hat{\theta}_i$ is a generic partonic variable to integrate (in our case, we have $\hat{\theta}_i = \hat{s}_1, \hat{s}_2, \hat{t}_1, \hat{t}_2$), we make the substitution

$$\theta_i = (\theta_{i+} - \theta_{i-})\,r_i + \theta_{i-}, \tag{3.32}$$

where $r_i$, $i = 3, 4, 5, 6$ are the random numbers given by VEGAS and are indeed in the right range: $r_i \in [0, 1]$ and $\theta_{i+}$, $\theta_{i-}$ are the old limits of integration. Of course we have to remember that this change of variables brings a factor given by the Jacobian of the transformation, which in this case is

$$J_2 = (\hat{s}_{2+} - \hat{s}_{2-})(\hat{t}_{1+} - \hat{t}_{1-})(\hat{t}_{2+} - \hat{t}_{2-})(\hat{s}_{1+} - \hat{s}_{1-}). \tag{3.33}$$

In our notation, the prefactor of the partonic cross section is:

$$\frac{1}{2E_1}\frac{1}{2E_2}\frac{1}{|\overline{v_1}-\overline{v_2}|}=\frac{1}{2\hat{s}}. \tag{3.34}$$

We then denote the prefactor of the hadronic cross section as:

$$L=\ln(\tau)\ln(\tau_1)f_1(x,\mu_F)f_2(\tau/x,\mu_F). \tag{3.35}$$

So the final expression will be:

$$\sigma=\int_0^1 dr_1\int_0^1 dr_2\int_0^1 dr_3\int_0^1 dr_4\int_0^1 dr_5\int_0^1 dr_6\frac{L\ J_1 J_2\left|\overline{\mathcal{A}}\right|^2}{512\pi^4\hat{s}^2(\hat{s}_2+\hat{t}_1-m_H^2))}. \tag{3.36}$$

# Chapter 4

# Amplitude

In this section, we describe the method used to find the amplitude of Triple-Higgs Production via Gluon Fusion at Leading Order.

## 4.1 General properties

We begin the study of the process by introducing the main features of the associated Feynman amplitude.

The amplitude of

$$g_\mu^a(p_1) + g_\nu^b(p_2) \to H(p_3) + H(p_4) + H(p_5) \tag{4.1}$$

is defined as:

$$\mathcal{A} = \frac{\alpha_S(\mu_R)}{2\pi} \frac{G_F m_H}{\sqrt{2}} \epsilon_\mu^a(p_1)\epsilon_\nu^b(p_2)\delta_{ab}\hat{\mathcal{A}}^{\mu\nu}(p_1, p_2, p_3, p_4), \tag{4.2}$$

where $\alpha_S(\mu_R)$ is the strong coupling constant defined at a renormalization scale $\mu_R$, $G_F$ is the Fermi Constant, $m_t$ is the top quark mass, and $\epsilon_\mu^a(p_1)\epsilon_\nu^b(p_2)$ are the polarization vectors of the two initial gluons.

Using this notation, all the information about the Lorentz structure of the amplitude is encoded in the tensor $\hat{\mathcal{A}}^{\mu\nu}(p_1, p_2, p_3, p_4)$. The latter tensor doesn't depend on the momentum $p_5$ since we implicitly used the 4-momentum conservation law:

$$p_5 = p_1 + p_2 - p_3 - p_4. \tag{4.3}$$

Moreover, the gluons are transversely polarised, so their momentum is perpendicular to their polarization vector, namely:

$$\epsilon^a(p_1) \cdot p_1 = 0, \quad \epsilon^b(p_2) \cdot p_2 = 0. \tag{4.4}$$

Also, the Ward identities have to be respected:

$$p_{1,\mu}\hat{\mathcal{A}}^{\mu\nu}(p_1, p_2, p_3, p_4) = 0, \quad p_{2,\nu}\hat{\mathcal{A}}^{\mu\nu}(p_1, p_2, p_3, p_4) = 0. \tag{4.5}$$

Finally, the amplitude must also respect Bose Symmetry for the interchange of the initial gluons $(\mu \leftrightarrow \nu, a \leftrightarrow b, p_1 \leftrightarrow p_2)$, so:

$$\hat{\mathcal{A}}^{\mu\nu}(p_1, p_2, p_3, p_4) = \hat{\mathcal{A}}^{\nu\mu}(p_2, p_1, p_3, p_4). \tag{4.6}$$

## 4.2 Projectors

The tensor $\hat{\mathcal{A}}^{\mu\nu}$ can be decomposed along a basis of projectors $\hat{\mathcal{T}}^{\mu\nu}$:

$$\hat{\mathcal{A}}^{\mu\nu} = \sum_n a_n(\hat{s}, \hat{s}_1, \hat{s}_2, \hat{t}_1, \hat{t}_2, m_t, m_H)\hat{\mathcal{T}}_n^{\mu\nu}, \tag{4.7}$$

where $a_n(\hat{s}, \hat{s}_1, \hat{s}_2, \hat{t}_1, \hat{t}_2, m_t, m_H)$ are scalar form factors. It can be noticed that we traded the dependence on the generic 4-momenta with the masses involved in the problem and the generalized Mandelstam variables defined in chapter 3.

In order to correctly construct the projectors we have to employ the symmetries discussed above.

First, the tensor structures with two indexes that respect Lorentz symmetry are only of three types:

- combinations of 4-momenta, i.e. $p_i^\mu p_j^\nu$, $i, j = 1, 2, 3, 4$;

- the metric tensor $g^{\mu\nu} = \mathrm{diag}(1, -1, -1, -1)$;

- the Levi-Civita tensor contracted in turn with two momenta, i.e. $\epsilon_{\rho\sigma}^{\mu\nu}p_i^\rho p_j^\sigma$, $i, j = 1, 2, 3, 4$.

The latter cannot be present because the interaction between fermions and gluons are vector-like in the SM Lagrangian (from a computational point of view, this can be seen from the fact that the $\epsilon$-tensor only comes out when we have traces involving $\gamma_5$, not present here).

So the tensor amplitude is written as the most general sum of all these Lorentz structures:

$$\hat{\mathcal{A}}^{\mu\nu} = a_1 g^{\mu\nu} + \sum_{i,j=1}^{4} a_{ij} p_i^\mu p_j^\nu. \tag{4.8}$$

However, the gluons are transversely polarized, and we have to keep in mind that this structures will be contracted with the two gluon polarization vectors. Since we arbitrarily chose $\epsilon_\mu^a(p_1)$ for the first gluon and $\epsilon_\nu^b(p_2)$ for the second one, everytime a projector will contain either $p_1^\mu$ or $p_2^\nu$, it will vanish upon contraction with one of the polarization vectors.

Therefore, the projectors will be constructed using only $p_1^\nu$ and $p_2^\mu$. With this in mind, the tensor amplitude can then be written as:

$$\begin{aligned}\hat{\mathcal{A}}^{\mu\nu} = {} & a_1 g^{\mu\nu} + a_2 p_2^\mu p_1^\nu + a_3 p_3^\mu p_1^\nu + a_4 p_4^\mu p_1^\nu + a_5 p_2^\mu p_3^\nu \\ & + a_6 p_2^\mu p_4^\nu + a_7 p_3^\mu p_3^\nu + a_8 p_3^\mu p_4^\nu + a_9 p_4^\mu p_3^\nu + a_{10} p_4^\mu p_4^\nu.\end{aligned} \tag{4.9}$$

We are then left with ten Lorentz structures with relative form factors $a_i$. We can still use gauge invariance. This means that the tensor amplitude needs to vanish if we contract it with $p_1^\mu$ or $p_2^\nu$. In practice, we get 6 conditions for the form factors:

$$\begin{cases} p_{1,\mu}p_{1,\nu}\hat{\mathcal{A}}^{\mu\nu} = 0 \\ p_{1,\mu}p_{2,\nu}\hat{\mathcal{A}}^{\mu\nu} = 0 \\ p_{1,\mu}p_{3,\nu}\hat{\mathcal{A}}^{\mu\nu} = 0 \end{cases} , \quad \begin{cases} p_{1,\mu}p_{4,\nu}\hat{\mathcal{A}}^{\mu\nu} = 0 \\ p_{3,\mu}p_{2,\nu}\hat{\mathcal{A}}^{\mu\nu} = 0 \\ p_{4,\mu}p_{2,\nu}\hat{\mathcal{A}}^{\mu\nu} = 0 \end{cases} . \tag{4.10}$$

The solution is:

$$\begin{aligned} a_1 &= \frac{a_{10}\hat{t}_2\hat{u}_2 - a_2\hat{s}^2 - a_4\hat{s}\hat{u}_1 + a_8\hat{t}_1\hat{t}_2}{2\hat{s}}, \quad a_3 = \frac{a_4\hat{s}\hat{u}_1 - a_8\hat{t}_1\hat{t}_2 + a_9\hat{u}_1\hat{u}_2}{\hat{s}\hat{t}_1} \\ a_5 &= -\frac{a_4\hat{s} + a_9\hat{u}_2}{\hat{t}_1}, \quad a_6 = -\frac{a_{10}\hat{t}_2 + a_9\hat{u}_1}{\hat{s}}, \quad a_7 = -\frac{a_{10}\hat{u}_2 + a_8\hat{t}_1}{\hat{s}}. \end{aligned} \tag{4.11}$$

One of the equations turns out to be trivial, so we have 5 independent form factors at the end. $\hat{\mathcal{A}}^{\mu\nu}$ is then written as:

$$\hat{\mathcal{A}}^{\mu\nu} = \sum_{i=2,4,8,9,10} a_i \hat{\mathcal{D}}_i^{\mu\nu}, \tag{4.12}$$

where the new projectors $\hat{\mathcal{D}}_i^{\mu\nu}$ are combinations of the simple Lorentz structures discussed above (Eq. (4.9)).

Now we can apply the Gran-Schmidt procedure to "orthonormalise" the base constructed using the five independent projectors. We notice that one of them has zero norm, so it will not contribute to the amplitude and we discard it.

We are then left with four projectors, which means that we will have to calculate only four form factors:

$$\hat{\mathcal{A}}^{\mu\nu} = f_1 \hat{\mathcal{S}}_1^{\mu\nu} + f_2 \hat{\mathcal{S}}_2^{\mu\nu} + f_3 \hat{\mathcal{S}}_3^{\mu\nu} + f_4 \hat{\mathcal{S}}_4^{\mu\nu}. \tag{4.13}$$

The projectors are orthonormal in the sense that we can calculate the polarization sum of the squared amplitude simply taking the squared moduli of the form factors:

$$\sum_{POL} |\mathcal{A}|^2 \propto \sum_{POL} \epsilon_\mu(p_1)\epsilon_\nu(p_2)\epsilon_\rho^*(p_1)\epsilon_\sigma^*(p_2)\hat{\mathcal{A}}^{\mu\nu}\hat{\mathcal{A}}^{\rho\sigma*} =$$
$$(-g_{\mu\rho})(-g_{\nu\sigma})\sum_n f_n\hat{\mathcal{S}}_n^{\mu\nu}\sum_m f_m^*\hat{\mathcal{S}}_m^{\rho\sigma*} = \sum_n |f_n|^2, \tag{4.14}$$

$$\text{since } \hat{\mathcal{S}}_n^{\mu\nu}\hat{\mathcal{S}}_{m,\,\mu\nu} = \delta_{mn}. \tag{4.15}$$

We write here the first two projectors, the other two will be written in Appendix (A.2):

$$\hat{\mathcal{S}}_1^{\mu\nu} = g^{\mu\nu} - \frac{p_1^\nu p_2^\mu}{p_1 \cdot p_2}, \tag{4.16}$$

$$\hat{\mathcal{S}}_2^{\mu\nu} = g^{\mu\nu} + \frac{2p_3^\mu(p_3^\nu(p_1 \cdot p_2) - p_1^\nu(p_2 \cdot p_3)) + p_2^\mu(p_3^2 p_1^\nu - 2p_3^\nu(p_1 \cdot p_3))}{2(p_1 \cdot p_3)(p_2 \cdot p_3) - p_3^2(p_1 \cdot p_2)}. \tag{4.17}$$

## 4.3 Calculation of the form factors

In this section, we present the method used to calculate the form factors.

First, we discuss how the Feynman diagrams were generated; then we show how the loop integrals were calculated, before we present the results.

### 4.3.1 Generating the Feynman diagrams

The $gg \to HHH$ amplitude is calculated making use of *Mathematica*.

The amplitude at LO is loop induced, since there is no interaction vertex connecting gluons and Higgs bosons in the SM. In general loop integrals diverge, however, in this case, given the fact that we do not have tree-level diagrams means that we also do not have counterterms to absorb the divergent part of the amplitude. Therefore, since the SM is a UV-safe theory, the sum of all possible Feynman diagrams needs to be UV-finite by itself providing a powerful check of the computation.

The Feynman diagrams relevant for the process are generated using the *Mathematica* package *FeynArts* [32] and appear always with a fermionic loop (with loop momentum $k$), and can be divided by their topologies in three cathegories: triangle loops, box loops and pentagon loops. It is natural to decompose each form factor following this classification:

$$f_i = f_i^{\triangle} + f_i^{\square} + f_i^{\pentagon}, \quad \text{for } i = 1, 2, 3, 4. \tag{4.18}$$
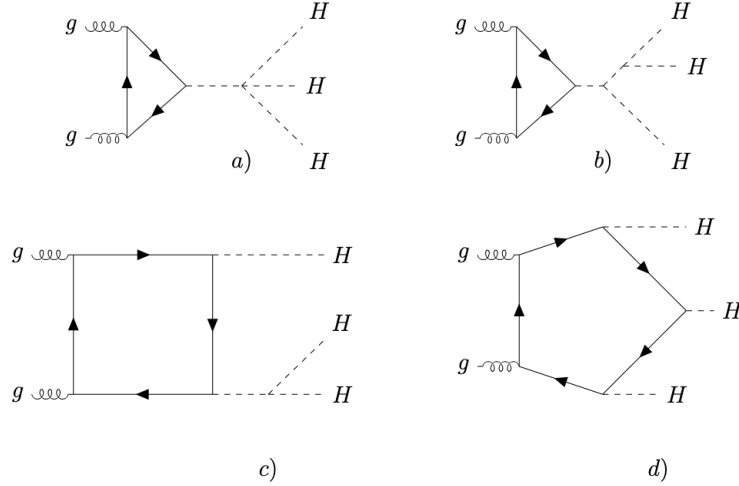
Figure 4.1: Feynman diagrams for triple Higgs production at leading order

Looking at Fig. 4.1 the Higgs self-couplings appear with different powers in the different topologies:

- The first triangle loop is attached to only one Higgs propagator that then splits into the three-Higgs final state through a quartic interaction. This class of diagrams will be proportional to the Higgs quartic self-coupling;

- The second triangle loop is instead attached to a chain of two Higgs propagators (this also means that it is very much suppressed relatively to all the others). This class of diagrams will be proportional to the Higgs triple self-coupling squared;

- The box loop is instead attached to a on-shell Higgs and Higgs propagator that then splits into two on-shell Higgs. This class of diagrams will be proportional to the triple Higgs self-coupling;

- The pentagon loop is directly attached to three on shell-Higgs bosons, without presenting any Higgs self-coupling.

The calculation is performed separately for each topology (triangle, box, and pentagon), so it is possible to keep track of the relative contribution of each to the total cross section.

Moreover, the triangle and box loops can be calculated more easily looking at single and double Higgs production, and then multiply the missing factors that come from the Higgs propagators and self-couplings. Doing so also allows one to have a powerful check with results available in the literature from single [33] and double Higgs production [34, 35].

In order to respect chirality conservation, the amplitude directly depends on positive powers of the mass of the quark running in the loop. This means that the top quark loop will give the largest contribution, so we turn off the masses of the other quarks in this thesis (this is also justified *a posteriori* since we checked that the contribution from bottom quark loops give a contribution under the 0.1% to the total cross section).

### 4.3.2   Loop Integral decomposition

After the generation of the diagrams, Dirac and color algebra is reduced using the *Mathematica* package *FeynCalc* [36–38].

The regularization scheme used in this work is dimensional regularization [39], which consists of

going from four space-time dimensions to $D = 4 - 2\epsilon$ spacetime dimensions, and then take the $\epsilon \to 0$ limit after the evaluation of the loop integrals. So we change the space-time dimensions of the amplitude using *FeynCalc*.

The fact that the projectors $\hat{S}_n^{\mu\nu}$ are orthonormal, means that it is very easy to isolate the single form factors.

The $i$-th form factor is in fact found simply by contracting the whole amplitude with the $i$-th propagator:

$$f_i = \hat{S}_i^{\mu\nu} \hat{A}_{\mu\nu}. \tag{4.19}$$

Dealing with scalar form factors instead of the tensor amplitude makes the computation much faster. However, one-loop integrals could be in principle always be solved even if tensorial. They are in fact reduced to a basis of scalar known functions through the Passarino-Veltman reduction scheme [40].

Starting from the generic one-loop tensor integral, classified by the number of propagator factors at the denominator $n$, and by the number of integration momenta $p$:

$$T_n^{\mu_1...\mu_p} = \frac{(2\pi\mu)^{4-D}}{i\pi^2} \int d^D k \frac{k^{\mu_1...\mu_p}}{D_0 D_1...D_{n-1}}, \quad D_i = (k + r_i)^2 - m_i^2 + i\epsilon. \tag{4.20}$$

The momenta follow the convention in figure 4.2.

For later purpose, we explicitly write four of those integrals following the usual notation, which consists of denoting $T_n$ with the $n$-th letter of the alphabet:

$$B^\mu = \frac{(2\pi\mu)^{4-D}}{i\pi^2} \int d^D k \, k^\mu \prod_{i=0}^{1} \frac{1}{(k + r_i)^2 - m_i^2}; \tag{4.21}$$

$$B^{\mu\nu} = \frac{(2\pi\mu)^{4-D}}{i\pi^2} \int d^D k \, k^\mu k^\nu \prod_{i=0}^{1} \frac{1}{(k + r_i)^2 - m_i^2}; \tag{4.22}$$

$$C^\mu = \frac{(2\pi\mu)^{4-D}}{i\pi^2} \int d^D k \, k^\mu \prod_{i=0}^{2} \frac{1}{(k + r_i)^2 - m_i^2}; \tag{4.23}$$

$$C^{\mu\nu} = \frac{(2\pi\mu)^{4-D}}{i\pi^2} \int d^D k \, k^\mu k^\nu \prod_{i=0}^{2} \frac{1}{(k + r_i)^2 - m_i^2}; \tag{4.24}$$
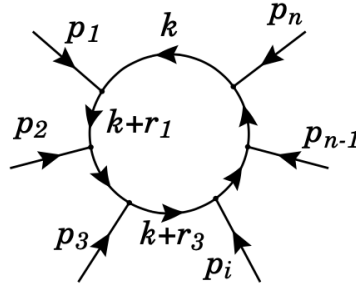


Figure 4.2: Momenta conventions for loop integrals

$$r_j = \sum_{i=1}^{j} p_i, \quad j = 1, ..., n - 1, \quad r_0 = 0. \tag{4.25}$$

25

The Passarino-Veltmann (PV) scalar integrals deserve a special mention. Indeed, it can be shown that the independent scalar integrals are only four, with these expressions [41]:

$$A_0[m_0^2] = \frac{(2\pi\mu)^{4-D}}{i\pi^2} \int d^D k \frac{1}{k^2 - m_0^2}, \tag{4.26}$$

$$B_0[r_{10}^2, m_0^2, m_1^2] = \frac{(2\pi\mu)^{4-D}}{i\pi^2} \int d^D k \prod_{i=0}^{1} \frac{1}{(k+r_i)^2 - m_i^2}, \tag{4.27}$$

$$C_0[r_{10}^2, r_{12}^2, r_{20}^2, m_0^2, m_1^2, m_2^2] = \frac{(2\pi\mu)^{4-D}}{i\pi^2} \int d^D k \prod_{i=0}^{2} \frac{1}{(k+r_i)^2 - m_i^2}, \tag{4.28}$$

$$D_0[r_{10}^2, r_{12}^2, r_{23}^2, r_{30}^2, r_{20}^2, r_{13}^2, m_0^2, m_1^2, m_2^2, m_3^2] = \frac{(2\pi\mu)^{4-D}}{i\pi^2} \int d^D k \prod_{i=0}^{3} \frac{1}{(k+r_i)^2 - m_i^2}, \tag{4.29}$$

where

$$r_{ij}^2 = (r_i - r_j)^2. \tag{4.30}$$

Moreover, due to Lorentz invariance in $D$-dimensions, each of the tensor integrals $T_n^{\mu_1 \dots \mu_p}$ in Eq. (4.20) can be decomposed as follows:

$$T_n^{\mu_1 \dots \mu_p} = \sum_i \Lambda_i^{\mu_1 \dots \mu_p} T_n^i, \tag{4.31}$$

where $\Lambda_i^{\mu_1 \dots \mu_p}$ are Lorentz invariant $p$-rank tensors that do not depend on the loop momentum and $T_n^i$ are scalar loop integrals with $n$ propagators. For example, Eq. (4.21) - (4.24) become:

$$B^\mu = r_1^\mu B_1; \tag{4.32}$$

$$B^{\mu\nu} = g^{\mu\nu} B_{00} + r_1^\mu r_1^\nu B_{11}; \tag{4.33}$$

$$C^\mu = r_1^\mu C_1 + r_2^\mu C_2; \tag{4.34}$$

$$C^{\mu\nu} = g^{\mu\nu} C_{00} + r_1^\mu r_1^\nu C_{11} + (r_1^\mu r_2^\nu + r_2^\mu r_1^\nu) C_{12} + r_2^\mu r_2^\nu C_{22}; \tag{4.35}$$

where $B_1$, $B_{00}$, $B_{11}$, $C_1$, $C_2$, $C_{00}$, $C_{11}$, $C_{12}$, $C_{22}$ are scalar integrals to be determined and are always combinations of the four independent ones written above. Basically, one can always write the tensor integral as a sum of scalar (and reducible) integrals times a Lorentz structure independent of the loop momentum. This step is called the Tensor Integral Decomposition (TID) and it is not unique, it depends on the conventions of Fig. 4.2.

To find the expressions of the reducible scalar integrals in terms of the four independent ones, in this thesis, we use the algorithm implemented in *FeynCalc*.

In order to illustrate the algorithm, in the following, we will consider the expression of the triangle loops as generated by *FeynArts* (before the contraction with the projector), the loop integral has the following expression:

$$T_3^{\mu\nu} = \int \frac{d^D k}{i\pi^2} \frac{g^{\mu\nu}(-2k^2 + 2m_t^2 - \hat{s}) + 4k^\mu k^\nu - 2p_1^\mu p_2^\nu + 2p_1^\nu p_2^\mu}{(k^2 - m_t^2)((k - p_1)^2 - m_t^2)((k + p_2)^2 - m_t^2)}. \tag{4.36}$$

The decomposition in terms of Eq. (4.20) integrals becomes clearer if we divide it into three terms:

$$T_3^{\mu\nu} = \int \frac{d^D k}{i\pi^2} \frac{g^{\mu\nu}(2m_t^2 - \hat{s}) + 2p_1^\nu p_2^\mu - 2p_1^\mu p_2^\nu}{(k^2 - m_t^2)((k-p_1)^2 - m_t^2)((k+p_2)^2 - m_t^2)}$$

$$+ \int \frac{d^D k}{i\pi^2} \frac{4k^\mu k^\nu}{(k^2 - m_t^2)((k-p_1)^2 - m_t^2)((k+p_2)^2 - m_t^2)} \tag{4.37}$$

$$+ \int \frac{d^D k}{i\pi^2} \frac{-2k^2 g^{\mu\nu}}{(k^2 - m_t^2)((k-p_1)^2 - m_t^2)((k+p_2)^2 - m_t^2)}.$$

The first two terms in Eq. (4.37) can already be written as PV functions, so we arrive at:

$$T_3^{\mu\nu} = (g^{\mu\nu}(2m_t^2 - \hat{s}) + 2p_1^\nu p_2^\mu - 2p_1^\mu p_2^\nu)C_0\left[p_1^2, p_2^2, (p_1+p_2)^2, m_t^2, m_t^2, m_t^2\right]$$

$$+ 4C^{\mu\nu}\left[p_1^2, p_2^2, (p_1+p_2)^2, m_t^2, m_t^2, m_t^2\right] \tag{4.38}$$

$$- 2g^{\mu\nu} \int \frac{d^D k}{i\pi^2} \frac{k^2}{(k^2 - m_t^2)((k-p_1)^2 - m_t^2)((k+p_2)^2 - m_t^2)}.$$

The last term of Eq. (4.38) can be decomposed in this way:

$$\int \frac{d^D k}{i\pi^2} \frac{k^2}{(k^2 - m_t^2)((k-p_1)^2 - m_t^2)((k+p_2)^2 - m_t^2)} =$$

$$= \int \frac{d^D k}{i\pi^2} \frac{k^2 - m_t^2 + m_t^2}{(k^2 - m_t^2)((k-p_1)^2 - m_t^2)((k+p_2)^2 - m_t^2)} = \tag{4.39}$$

$$= B_0[(p_1+p_2)^2, m_t^2, m_t^2] + m_t^2 C_0[p_1^2, p_2^2, (p_1+p_2)^2, m_t^2, m_t^2, m_t^2];$$

where in the first step we added and subtracted $m_t^2$ and split the integral in two pieces. We can then simplify $(k^2 - m_t^2)$ with one denominator and get a function $B_0[\hat{s}, m_t^2, m_t^2]$. The second one, of course, is precisely the function $C_0[0, 0, \hat{s}, m_t^2, m_t^2, m_t^2]$ times $m_t^2$, where we simplified the scalar products because we implicitly went back to 4-dimension. In a real calculation, this must be done with care in order to correctly deal with the divergent part of the $B_0$ functions.

$$\Rightarrow T_3^{\mu\nu} = (g^{\mu\nu}(2m_t^2 - \hat{s}) + 2p_1^\nu p_2^\mu - 2p_1^\mu p_2^\nu)C_0\left[0, 0, \hat{s}, m_t^2, m_t^2, m_t^2\right]$$

$$+ 4C^{\mu\nu}\left[0, 0, \hat{s}, m_t^2, m_t^2, m_t^2\right] - 2g^{\mu\nu}(B_0[\hat{s}, m_t^2, m_t^2] + m_t^2 C_0[0, 0, \hat{s}, m_t^2, m_t^2, m_t^2]). \tag{4.40}$$

Let us turn to the decomposition of the remaining tensor integral $C^{\mu\nu}$. We start from Eq. (4.35):

$$C^{\mu\nu} = g^{\mu\nu}C_{00} + p_1^\mu p_1^\nu C_{11} + (p_1^\mu p_2^\nu + p_2^\mu p_1^\nu)C_{12} + p_2^\mu p_2^\nu C_{22}. \tag{4.41}$$

The only thing left to do is to find the coefficients $C_{ij}$ in terms of the independent set of scalar integrals (Eq. (4.21)-(4.24)). To do so, we contract $C^{\mu\nu}$ with the Lorentz structures at our disposal, $p_1^\mu$, $p_1^\nu$, $p_2^\mu$, $p_2^\nu$, and $g^{\mu\nu}$:

$$g_{\mu\nu}C^{\mu\nu} = 4C_{00} + C_{11}p_1^2 + 2C_{12}(p_1 \cdot p_2) + p_2^2 C_{22}. \qquad (4.42)$$

On the other hand, $C^{\mu\nu}$ can be written in terms of the loop momentum combination $k^\mu k^\nu$ as in Eq. (4.24), so Eq. (4.42) is also equal to:

$$g_{\mu\nu}C^{\mu\nu} = g_{\mu\nu} \int \frac{d^D k}{i\pi^2} \frac{k^\mu k^\nu}{D_0 D_1 D_2} = \int \frac{d^D k}{i\pi^2} \frac{k^2}{(k^2 - m_t^2)((k - p_1)^2 - m_t^2)((k + p_2)^2 - m_t^2)} \qquad (4.43)$$

$$= B_0[p_1^2 + 2p_1 \cdot p_2 + p_2^2, m_t^2, m_t^2] + m_t^2 C_0[p_1^2, p_2^2, [p_1^2 + 2p_1 \cdot p_2 + p_2^2, m_t^2, m_t^2, m_t^2].$$

Now we can equate Eq. (4.42) with Eq. (4.43) to get a condition on the $C_{ij}$.
If we follow the same method substituting $g^{\mu\nu}$ in turn with $p_1^\mu p_1^\nu$, $p_1^\mu p_2^\nu$ and $p_2^\mu p_2^\nu$, we obtain a system of four equations in four variables that allows to uniquely determine the $C_{ij}$ in terms of $B_0$ and $C_0$ functions.
*FeynCalc* gives the possibility to do the whole PV decomposition with a few lines of code, so we apply it to each form factor, always keeping distinct the different contributions coming from different topologies.
We also have pentagon diagrams, so we also have to deal with the 5-point scalar functions $E_0$.

$$E_0[r_{10}^2, r_{12}^2, r_{23}^2, r_{34}^2, r_{40}^2, r_{30}^2, r_{20}^2, r_{13}^2, r_{14}^2, r_{24}^2, m_0^2, m_1^2, m_2^2, m_3^2, m_4^2] =$$
$$= \frac{(2\pi\mu)^{4-D}}{i\pi^2} \int d^D k \prod_{i=0}^{4} \frac{1}{(k + r_i)^2 - m_i^2}. \qquad (4.44)$$

The package used to numerically evaluate the scalar integrals, *LoopTools* [42, 43], contains also a library for them, even though they can always be expressed as linear combinations of $D_0$ functions when going back to 4 dimensions [44].
At this point we check that each form factor is indeed UV finite as we expect. In dimensional regularization, the UV divergent terms will be the ones proportional to the pole $1/\epsilon$. So we explicitly write:

$$D = 4 - 2\epsilon,$$

and we explicitate the pole structure of the $B_0$ function as follows:

$$B_0[q, m_t^2, m_t^2] = \frac{1}{\epsilon} + B_0^{\text{fin}}[q, m_t^2, m_t^2],$$

where $B_0^{\text{fin}}$ is the UV-safe part of the $B_0$. Only now do we take the $\epsilon \to 0$ limit and we stop at the 0-th order namely $\mathcal{O}(\epsilon^0)$. Now we check that the amplitude is not UV divergent looking for the coefficient of $1/\epsilon$, which is zero for all three topologies of each form factor separately.
Finally, we have an expression for all the form factors that depend only on the mass scales of the problem $m_t$, $m_h$, on the Mandelstam variables $\hat{s}$, $\hat{s}_1$, $\hat{s}_2$, $\hat{t}_1$, $\hat{t}_2$, and on the known scalar PV functions $B_0^{\text{fin}}$, $C_0$, $D_0$ and $E_0$.
We store each topology contribution to each form factor into a separate subroutine. To translate them to FORTRAN language we use the *Mathematica* package *FormCalc* [45]. Despite the complexity and size of the expressions of the form factors, our Montecarlo-code proved to be stable and efficient in numerically evaluating the multidimensional integrals.

### 4.3.3 Results

We now need to take the squared modulus of the amplitude, to get the last piece to calculate the cross section.

To get the unpolarized squared amplitude, we have to sum over all external polarizations and average over the initial ones and over color.

Being a massless vector field, the gluon has two polarizations and, being charged under $SU(3)_C$, 8 degrees of freedom of color, so we have to average over those for both gluons. The sum over the external polarizations was already discussed in Eq. (4.14), the only missing ingredient is a factor of 8 coming from the $SU(3)_C$ algebra:

$$\left|\overline{\mathcal{A}}\right|^2 = \frac{1}{2}\frac{1}{2}\frac{1}{8}\frac{1}{8}8\frac{\alpha_S^2(\mu_R)}{(2\pi)^2}\frac{G_F^2 m_H^2}{2}\sum_i |f_i|^2. \tag{4.45}$$

For the numerical calculation we used the following set of parameters:

$$G_F = 1.664 \times 10^{-5} \text{ GeV}^{-2}, \quad m_H = 125.0 \text{ GeV}, \quad m_W = 80.4 \text{ GeV}, \tag{4.46}$$

$$m_t = 173.0 \text{ GeV}, \quad m_b = 0. \tag{4.47}$$

For the strong coupling constant $\alpha_s(\mu)$, we assumed the factorization and the renormalization scales to be the same ($\mu_R = \mu_F = \mu$), and chose $\mu = \frac{\sqrt{\hat{s}}}{2}$.
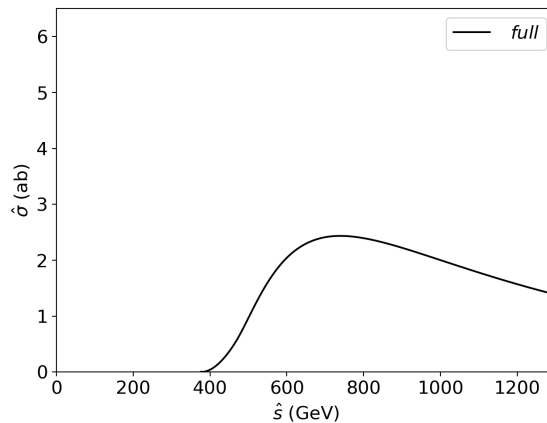


Figure 4.3: Full partonic cross section as a function of the partonic CoM energy.

In Fig. 4.3 the full partonic cross section in attobarn is shown as a function of the partonic center of mass energy in GeV.

It is useful to look at the contributions from the different topologies, so we decompose the partonic cross section $\hat{\sigma}$ in analogy to what was done for the form factors in Eq. (4.18)

$$\hat{\sigma} = \hat{\sigma}^{\triangle} + \hat{\sigma}^{\square} + \hat{\sigma}^{\hexagon} + \hat{\sigma}^{\text{int}}, \tag{4.48}$$

where $\hat{\sigma}^{\text{int}}$ comes from the interference between the topologies. In practice, we calculate the partonic cross section in our code turning on only the relevant topology for each form factor and setting all the other contributions to zero. The result is shown in the plot in Fig. 4.4.

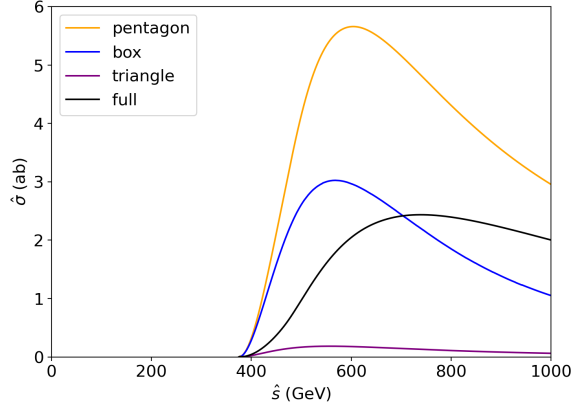Figure 4.4: Different topologies contributions to the partonic cross section as a function of the partonic CoM energy.

Looking at Fig. 4.4, the triangle topology gives the smallest contribution. This was expected since the Feynman diagrams with triangle loops are the most suppressed by Higgs propagators. We can also infer that there is a large destructive interference, since the total cross section in Fig. 4.4 is smaller if compared to the contributions of the single topologies.

Another interesting result to point out is the different contributions to the partonic cross section coming from different form factor.

So we plot the partonic cross section as a function of the partonic center of mass energy turning on one form factor at a time (like we did for the topologies), the only difference is that this time we do not have any interference terms since we chose to work with orthonormal projectors.
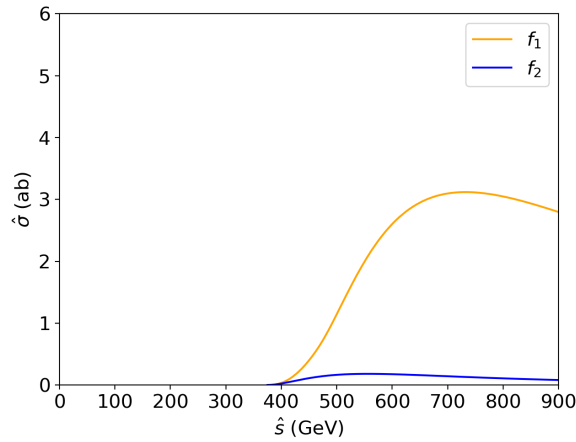


Figure 4.5: Form factors contribution to the partonic cross section as a function of the partonic CoM energy.

We show the contributions from the form factors in Fig. 4.5.

Clearly, the first form factor dominates over the others. In particular, the third and fourth ones are completely negligible giving a contribution of ten orders of magnitude less than the first one, whereas the second one is not as small and gives a sizeable contribution, as can be seen from Fig. 4.6.
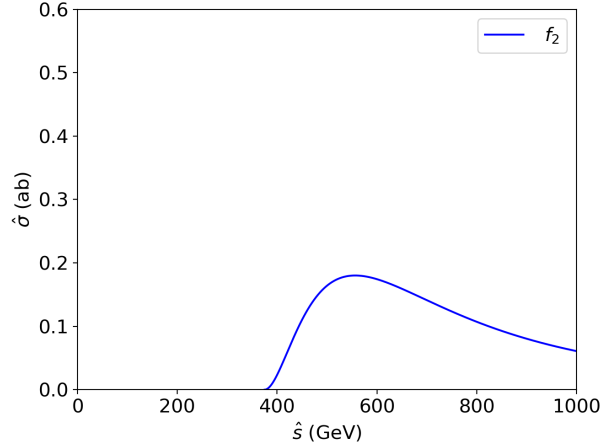
Figure 4.6: Zoom on the second form factor contribution to the partonic cross section as a function of the partonic CoM energy.

Now we turn our attention to the hadronic cross section. As pointed out earlier, we used the set `NNPDF40-lo-as-01180` [26] from LHAPDF [25] for the PDFs.

The final results are shown in Table 4.1, where the first line refers to the maximum center of mass energy at the LHC. The other two refer to higher energies, not accessible at the moment, and serve only as reference values. The uncertainties reflect the ones obtained from the Monte Carlo integration error.

| $E_{CM}$(TeV) | $\sigma$ (ab) |
|---|---|
| 14 | 24.88±0.05 |
| 27 | 126.4±0.1 |
| 100 | 1690±5 |

Table 4.1: Hadronic cross section of triple Higgs production at the LHC for different COM energies.

Reference [14] also presents the cross section of triple-Higgs production at the LHC, but the results are slightly different from the ones shown in Table 4.1. This can be explained by the fact that Ref. [14] used an older PDF set and a constant value for the strong coupling constant ($\alpha_S = 0.138$). We checked that the two results agree within the integration error using the same input parameters.

We can look at the hierarchy between the form factors and between the different topologies also for the hadronic cross section.

We notice that the third and fourth form factors are very suppressed (10 orders of magnitude less than the others), so they are *numerically* compatible with zero. Unfortunately, we could not demonstrate that they vanish analytically due to the complexity of the symbolic expressions.

Looking at Table 4.2 and Table 4.3, we see that the hierarchies found earlier for the partonic cross section hold also at the hadronic cross section level, both for the different topologies and for the two form factors. This is not surprising since the hierarchy holds for the whole range of partonic center-of-mass energies.

31

| $E_{CM}$(TeV) | $\sigma_1$ (ab) | $\sigma_2$ (ab) |
|:---:|:---:|:---:|
| 14 | 24.88±0.05 | $0.250 \pm 0.002$ |
| 27 | 126.4±0.1 | $1.45 \pm 0.03$ |
| 100 | 1690±5 | $22.2 \pm 0.1$ |

Table 4.2: Contributions to the hadronic cross section of triple Higgs production at the LHC for different COM energies from the two relevant form factors.

| $E_{CM}$(TeV) | $\sigma^{\triangle}$ (ab) | $\sigma^{\square}$ (ab) | $\sigma^{\pentagon}$ (ab) |
|:---:|:---:|:---:|:---:|
| 14 | $0.090 \pm 0.003$ | $34.20 \pm 0.05$ | $61.0 \pm 0.2$ |
| 27 | $0.44 \pm 0.01$ | $160.0 \pm 0.2$ | $293.0 \pm 0.3$ |
| 100 | $5.50 \pm 0.01$ | $1910 \pm 3$ | $3620 \pm 5$ |

Table 4.3: Contributions to the hadronic cross section of triple Higgs production at the LHC for different COM energies from the different topologies.

# Chapter 5

# The transverse momentum expansion

In this chapter, we are going to present the transverse momentum ($p_t$) expansion of the amplitude.

In the first section, we will describe the expansion in the forward limit, in the second section we will discuss how to solve the loop integrals after the expansion, and in the last we will present the results.

## 5.1 Description of the expansion

The purpose of the expansion was to reduce the number of energy scales involved in the integrals. Triangle loop integrals do not need an expansion since they are already expressed in terms of one energy scale.

It is convenient to expand the box and pentagon topologies separately, so we first present the expansion for the pentagon loop integrals, and afterwards, the one used for the box integrals.

### 5.1.1 Pentagon diagrams

Here we will focus on the expansion of the pentagon loops.

From now on, it is more convenient to use the set of kinematical variables $(\hat{s}, \hat{t}_1, \hat{t}_2, \hat{s}'_1, \hat{s}'_2)$, where $\hat{s}, \hat{t}_1, \hat{t}_2$ have already been defined in Eq. (3.8), and $\hat{s}'_i$ are defined as:

$$\hat{s}'_1 = -2p_3 \cdot p_5, \quad \hat{s}'_2 = -2p_4 \cdot p_5. \tag{5.1}$$

The kinematical quantities relevant for this expansion are the Higgs transverse momenta which, assuming the gluons travel along the $z$-axis, are defined as:

$$p_{t,3} = \sqrt{p_{3x}^2 + p_{3y}^2}, \quad p_{t,4} = \sqrt{p_{4x}^2 + p_{4y}^2}, \tag{5.2}$$

and are expressed in terms of the kinematical variables as:

$$p_{t,3}^2 = m_H^2 - \frac{\hat{t}_1 \hat{u}_1}{s}, \quad p_{t,4}^2 = m_H^2 - \frac{\hat{t}_2 \hat{u}_2}{s}, \tag{5.3}$$

where $\hat{u}_1$ and $\hat{u}_2$ were defined in Eq. (3.9) and depend on $\hat{s}'_1, \hat{s}'_2$ in the following way:

$$\hat{u}_1 = 2p_2 \cdot p_3 = \hat{s} + \hat{s}'_2 - \hat{t}_1 - m_H^2, \tag{5.4}$$

$$\hat{u}_1 = 2p_1 \cdot p_4 = \hat{s} + \hat{s}'_1 - \hat{t}_2 - m_H^2. \tag{5.5}$$

The transverse momenta can be found by decomposing $p_3$ and $p_4$ in terms of a part parallel to the beam axis (so proportional to $p_1$ and $p_2$), and a part perpendicular to it, that we denote with $r_{3,\perp}$ and $r_{4,\perp}$. So we have:

$$\begin{cases} p_3^\mu = a_3 p_1^\mu + b_3 p_2^\mu + r_{3,\perp}^\mu \\ p_4^\mu = a_4 p_1^\mu + b_4 p_2^\mu + r_{4,\perp}^\mu, \end{cases} \tag{5.6}$$

where $a_3$, $a_4$, $b_3$, $b_4$ are coefficients to be determined and, in order to have

$$p_1 \cdot r_{3,\perp} = p_1 \cdot r_{4,\perp} = p_2 \cdot r_{3,\perp} = p_2 \cdot r_{4,\perp} = 0 \tag{5.7}$$

we need

$$r_{3,\perp} = (0; p_{3x}, p_{3y}, 0), r_{4,\perp} = (0; p_{4x}, p_{4y}, 0). \tag{5.8}$$

Therefore, taking the square of these "perpendicular" momenta we get the transverse momenta, with a minus sign that shows that $r_{3,\perp}$ and $r_{4,\perp}$ are space-like:

$$r_{3,\perp}^2 = -p_{t,3}^2, \quad r_{4,\perp}^2 = -p_{t,4}^2. \tag{5.9}$$

The coefficients $a_i$ and $b_i$ ($i = 3, 4$) are found by contracting Eq. (5.6) in turn with $p_1$ and $p_2$:

$$\begin{cases} \frac{\hat{t}_1}{2} = p_1 \cdot p_3 = a_3 p_1 \cdot p_1 + b_4 p_1 \cdot p_2 + p_1 \cdot r_{3,\perp} = b_3 \frac{\hat{s}}{2} \\ \frac{\hat{u}_1}{2} = p_2 \cdot p_3 = a_3 p_2 \cdot p_1 + b_4 p_2 \cdot p_2 + p_2 \cdot r_{3,\perp} = a_3 \frac{\hat{s}}{2} \\ \frac{\hat{u}_2}{2} = p_1 \cdot p_4 = a_4 p_1 \cdot p_1 + b_4 p_1 \cdot p_2 + p_1 \cdot r_{4,\perp} = b_4 \frac{\hat{s}}{2} \\ \frac{\hat{t}_2}{2} = p_2 \cdot p_4 = a_4 p_2 \cdot p_1 + b_4 p_2 \cdot p_2 + p_2 \cdot r_{4,\perp} = a_4 \frac{\hat{s}}{2} \end{cases} \iff \begin{cases} a_3 = \frac{\hat{u}_1}{\hat{s}}, \quad b_3 = \frac{\hat{t}_1}{\hat{s}} \\ a_4 = \frac{\hat{t}_2}{\hat{s}}, \quad b_3 = \frac{\hat{u}_2}{\hat{s}} \end{cases} \tag{5.10}$$

So we get:

$$p_3^\mu = p_1^\mu - \frac{\hat{t}_1}{\hat{s}}(p_1^\mu - p_2^\mu) + \frac{\Delta_2}{\hat{s}} p_1^\mu + r_{3,\perp}^\mu, \tag{5.11}$$

$$p_4^\mu = p_2^\mu - \frac{\hat{t}_2}{\hat{s}}(p_2^\mu - p_1^\mu) + \frac{\Delta_1}{\hat{s}} p_2^\mu + r_{4,\perp}^\mu,$$

where $\Delta_i = \hat{s}_i' - m_H^2$, for $i = 1, 2$.

Using this notation, we identify the forward limit as the configuration in which both $p_3^\mu \sim p_1^\mu$ and $p_4^\mu \sim p_2^\mu$ are respected. Looking at Eq. (5.11), this situation corresponds to:

$$\frac{\hat{t}_1}{\hat{s}} \ll 1, \quad \frac{\Delta_1}{\hat{s}} \ll 1, \quad \frac{\hat{t}_2}{\hat{s}} \ll 1, \quad \frac{\Delta_2}{\hat{s}} \ll 1, \quad r_{3,\perp}^\mu \sim 0^\mu, \quad r_{4,\perp}^\mu \sim 0^\mu. \tag{5.12}$$

It is useful to explicitly introduce the transverse momenta in the amplitude by solving the system of equation constructed with Eq. (5.3)–(5.5), to get $\hat{t}_1$ and $\hat{t}_2$ in terms of $\hat{s}_1'$, $\hat{s}_2'$, $p_{t,3}^2$, $p_{t,4}^2$:

$$\hat{t}_{1,\pm} = \frac{\hat{s}}{2} \left( 1 + \frac{\Delta_2}{\hat{s}} \pm \sqrt{\left(1 + \frac{\Delta_2}{\hat{s}}\right)^2 - 4 \frac{p_{t,3}^2 + m_H^2}{\hat{s}}} \right), \tag{5.13}$$

$$\hat{t}_{2,\pm} = \frac{\hat{s}}{2} \left( 1 + \frac{\Delta_1}{\hat{s}} \pm \sqrt{\left(1 + \frac{\Delta_1}{\hat{s}}\right)^2 - 4 \frac{p_{t,4}^2 + m_H^2}{\hat{s}}} \right), \tag{5.14}$$

The forward limit corresponds to the "negative" solutions $\hat{t}_{1,-}$, $\hat{t}_{2,-}$ and we can look at Eq. (5.13) and Eq. (5.14) to express the limits in Eq. (5.12) as (we also use the definitions of the $\Delta_i$):

$$\frac{p_{t,3}^2}{\hat{s}} \ll 1, \quad \frac{\hat{s}_1'}{\hat{s}} \ll 1, \quad \frac{p_{t,4}^2}{\hat{s}} \ll 1, \quad \frac{\hat{s}_2'}{\hat{s}} \ll 1, \quad \frac{m_H^2}{\hat{s}} \ll 1, \quad r_{3,\perp}^\mu \sim 0^\mu, \quad r_{4,\perp}^\mu \sim 0^\mu. \tag{5.15}$$

### 5.1.2 Box diagrams

Looking at Fig. 4.1, we can see that the box loop is connected with the final state through one on-shell Higgs boson, and one virtual Higgs line.

Hence, it is possible to calculate the box integral by studying Double Higgs production, but introducing different dummy masses for the final state. So we calculate the form factors of the diagram in Fig. 5.1 as before.
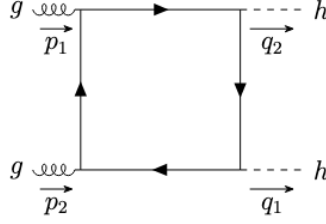


Figure 5.1: Box diagram in Double Higgs production.

We call the contribution it gives to each form factor $g_i^\square$, $i = 1, 2, 3, 4$. We set the masses of the final state particles to be:

$$q_1^2 = m_1^2, \quad q_2^2 = m_2^2, \tag{5.16}$$

and we exploit the conservation of momenutum:

$$q_2 = p_1 + p_2 - q_1. \tag{5.17}$$

The kinematical variables will be the reduced Mandelstam for 2→2 processes:

$$\hat{s}' = p_1 \cdot p_2, \quad \hat{t}' = p_1 \cdot q_1, \quad \hat{u}' = p_2 \cdot q_1, \tag{5.18}$$

where

$$\hat{s}' + \hat{t}' + \hat{u}' = \frac{m_1^2 - m_2^2}{2} = \Delta_m. \tag{5.19}$$

The transverse momentum $p_t$ of the particle with momentum $q_1$ is expressed in terms of the other kinematical variables as:

$$p_t^2 = 2\frac{\hat{t}'\hat{u}'}{\hat{s}'} - m_1^2. \tag{5.20}$$

We can express momentum $q_1$ in analogy to what we did in Eq. (5.6):

$$q_1^\mu = ap_1^\mu + p_2^\mu + r_\perp^\mu = p_1^\mu - \frac{\hat{t}'}{\hat{s}'}(p_1^\mu - p_2^\mu) + \frac{\Delta_m}{\hat{s}'}p_1^\mu + r_\perp^\mu, \tag{5.21}$$

where the coefficients $a$ and $b$ are found by contracting Eq. (5.21) in turn with $p_1^\mu$ and $p_2^\mu$, and $r_\perp^\mu$ is the part of $q_1^\mu$ perpendicular to the beam axis.

The forward limit is associated to the configuration where $p_1 \simeq q_1$, so Eq. (5.21) suggests one obtains it when:

$$\frac{\hat{t}'}{\hat{s}'} \ll 1, \qquad \frac{\Delta_m}{\hat{s}'} \ll 1, \qquad r_\perp^\mu \simeq 0^\mu \tag{5.22}$$

We can express $\hat{t}'$ and $\hat{u}'$ in terms of the transverse momentum by solving the system of two equations formed by Eq. (5.19) and Eq. (5.21).

In the forward limit we obtain:

$$\hat{t}' = \frac{\hat{s}'}{2} \left( 1 + \frac{\Delta_m}{\hat{s}'} - \sqrt{\left(1 + \frac{\Delta_m}{\hat{s}'}\right)^2 - 2\frac{p_t^2 + m_2^2}{\hat{s}'}} \right), \tag{5.23}$$

So we can express the conditions for the forward limit as:

$$\frac{p_t^2}{\hat{s}'} \ll 1, \quad \frac{m_1^2}{\hat{s}'} \ll 1, \quad \frac{m_2^2}{\hat{s}'} \ll 1, \quad r_\perp^\mu \sim 0^\mu, \tag{5.24}$$

After calculating the loop integrals (more on this later), we can easily recover all the Triple-Higgs box contribution to each form factor ($f_i^\square$, $i = 1, 2, 3, 4$).

The difference between the box diagrams in Fig. 5.1 and Fig. 4.1 is that one of the two final state lines splits into two on shell Higgs in the Triple Higgs case. So what is missing is one Higgs propagator and one power of the trilinear Higgs self coupling. So we reconstruct ($f_i^\square$, $i = 1, 2, 3, 4$) by multiplying the missing factors to $g_i^\square$:

$$f_i^\square \propto \frac{g_{3h}}{q_1^2 - m_H^2} g_i^\square, \qquad g_{3h} = \lambda v, \tag{5.25}$$

where $\lambda$ was defined in Eq. (2.41), and $v$ is the Higgs VEV.

We also have expressed the conservation of momentum in the trilinear vertex, and keep track of all the possible combinations of the final state particle rearranging:

$$f_i^\square = \sum_{(abc)} \frac{g_{3h}}{q_1^2 - m_H^2} g_i^\square \Bigg|_{\substack{q_1 = p_a + p_b \\ q_2 = p_c}} \tag{5.26}$$

where the sum is done over all different triplets $(abc)$, respectively, $(345), (354), (453)$.

The identification of $(q_1, q_2)$ in terms of $(p_3, p_4, p_5)$ has to be done also for Eq. (5.18) and Eq. (5.20) in order to express the final expression in terms of the Triple-Higgs kinematics.

### 5.1.3 Practical algorithm

It is useful to sketch the practical algorithm followed to expand the amplitude around the small parameters in Eq. (5.15).

We only do it for the pentagon diagrams since the analogy with the box diagrams is trivial and it was already done in the cited works above.

- In the beginning, we follow the same steps as before, so we generate the diagrams using *FeynArts*, then we use *FeynCalc* to contract them with the projectors to get the form factors. Afterwards, we simplify the Dirac and $SU(3)_C$ algebras and obtain a list of integrals that represent the starting point for the calculation.

- We substitute $p_5$ everywhere in the form factors using the momentum conservation law. Afterwards, we use Eq. (5.11) to express $p_3$ and $p_4$ everywhere in terms of $p_1$, $p_2$, $r_{3,\perp}$, $r_{4,\perp}$ and the kinematical variables. Then we use Eq. (5.13) and Eq. (5.14) to express $\hat{t}_i$ in terms of the transverse momenta.

- The integrands are now written only in terms of the quantities in Eq. (5.15), so we are ready to perform the expansion. It is done considering only two energy hierarchies: the small parameters (already defined) and the large parameters ($\hat{s}$ and $m_t^2$). Practically, all small parameters are rewritten as if they were multiplying a common scale $x$. Then we

Taylor expand the form factors around $x = 0$ and put $x = 1$ after the expansion. In order to be consistent, we must take into account the different dimensionalities of the parameters, so we scale them this way:

$$(r_{3,\perp}^\mu, r_{4,\perp}^\mu) \mapsto x \, (r_{3,\perp}^\mu, r_{4,\perp}^\mu), \quad (p_{t,3}^2, p_{t,4}^2, m_H^2, \hat{s}_1', \hat{s}_2') \mapsto x^2 \, (p_{t,3}^2, p_{t,4}^2, m_H^2, \hat{s}_1', \hat{s}_2'). \quad (5.27)$$

It must be emphasized that we must treat $r_{i,\perp}$ and $p_{t,i}$ as independent quantities even though we know that $r_{i,\perp}^2 = -p_{t,i}^2$ for $i = 3, 4$. This is because this expansion is performed before the loop integration, so we will have scalar products between the perpendicular momenta and the loop momentum and we need to use Eq. (5.27) to consistently deal with this issue.

Throughout the rest of this thesis, we will refer to a given order $n$ of the expansion as the $\mathcal{O}(p_t^{2n})$ term, but we are implicitly including all the terms scaling as $((\frac{a}{b})^n)$, where $a = m_H^2, p_{t,3}^2, p_{t,4}^2, \hat{s}_1', \hat{s}_2'$, and $b = \hat{s}, m_t^2$.

In analogy to the other works where the $p_t$ expansion was used [15, 17, 46], we expect it to hold in all the phase-space points with $\sqrt{\hat{s}} \le 4m_t \simeq 750$ GeV. We will check that roughly after this value, the approximated partonic cross section will start to depart from its exact value.

- At this point we can store each term of the Taylor expansion for each form factor to keep track of the expansion order. So we can solve the loop integrals. The standard PV decomposition proposed in *FeynCalc* fails in this context. In the next section we will explore in detail the method used to solve these kind of integrals.

- Now we can calculate the cross section exploiting the same integration technique as before.

The advantage of calculating the cross section in this way is that the integrals will depend only on one energy scale, namely $\hat{s}/m_t^2$, making them much faster to evaluate on our FORTRAN code. In particular, this will be of advantage when one goes to next-to-leading order (NLO), where the appearance of two-loop integrals with several mass scales can become very complicated.

We can see how this works with an example. Let's consider the following class of pentagon integrals, as they appear in our calculation:

$$\int d^D k \frac{(k \cdot p_1)^{a_1} (k \cdot p_2)^{a_2} (k \cdot p_3)^{a_3} (k \cdot p_4)^{a_4} (k^2)^{a_5}}{[k^2 - m_t^2] \, [(k + p_2)^2 - m_t^2] \, [(k - p_4)^2 - m_t^2] \, [(k + p_3)^2 - m_t^2] \, [(k - p_1)^2 - m_t^2]}, \quad (5.28)$$

where $a_i \ge 0$, $i \in [1, 5]$. The integral in Eq.(5.28) will depend only on the masses of propagators (only one in this case), and on the kinematical quantities formed by the external momenta. In total we have seven energy scales: $\hat{s}, \hat{s}_1', \hat{s}_2', \hat{t}_1, \hat{t}_2, m_H^2$ and $m_t^2$.

The $p_t$ expansion will modify the terms of Eq. (5.28) that contain $p_3$ or $p_4$, namely:

$$\frac{(k \cdot p_3)^{a_3} (k \cdot p_4)^{a_4}}{[(k - p_4)^2 - m_t^2] \, [(k + p_3)^2 - m_t^2]}. \quad (5.29)$$

Using Eq. (5.11),(5.13), (5.14), and expanding Eq. (5.29) in the forward limit, will generate terms like $k \cdot p_1$, $k \cdot p_2$, $k \cdot r_{3,\perp}$, $k \cdot r_{4,\perp}$ and other $(k^2 - m_t^2)$ factors in the denominator. Therefore, expanding the integrand in Eq. (5.28) results in:

$$\int d^D k \frac{(k \cdot p_1)^{a_1'} (k \cdot p_2)^{a_2'} (k \cdot r_{3,\perp})^{a_3'} (k \cdot r_{4,\perp})^{a_4'} (k^2)^{a_5}}{[k^2 - m_t^2]^n \, [(k - p_2)^2 - m_t^2] \, [(k + p_1)^2 - m_t^2]}, \quad (5.30)$$

where the $a_i'$ are new non-negative integers and $n$ is strictly positive. It is easy to see that these integrals will only depend on $\hat{s}, p_{t,3}^2, p_{t,3}^2, m_t^2$, so we already reduced the number of energy scales

with respect to the starting integral.

Moreover, since the perpendicular momenta $r_{i,\perp}$ appear only at the numerator, we can use the Integration-by-parts (IBP) relations to rewrite the integral in Eq. (5.30) in terms of integrals where $a_3' = 0 = a_4'$. This technique will be reviewed in the next section.

In the end, we will have a dependence on only the mass ratio $\hat{s}/m_t^2$.

## 5.2   IBP Reduction

In this section, we will briefly review the method used to solve the loop integrals after the $p_t$ expansion.

At the end, the form factors will still depend on the PV scalar functions because, as we stated before, one-loop integrals can always be decomposed along the basis of the four scalar integrals in Eq. (4.26)-(4.29). Doing so, one encounters though an issue with *LoopTools* when calculating the expanded loop integrals using the algorithm presented in Section 4.3.2.

As an example we show an integral as the one of Eq. (5.30), where $a_1' = a_2' = a_3' = a_4' = a_5 = 0$ and $n = 3$:

$$\int \mathrm{d}^D k \frac{1}{[k^2 - m_t^2]^3 \left[(k - p_1)^2 - m_t^2\right] \left[(k + p_2)^2 - m_t^2\right]}. \tag{5.31}$$

As a first instinct one would be considering it as a $E_0 \left[0, 0, 0, s, 0, 0, 0, 0, 0, 0, m_t^2, m_t^2, m_t^2, m_t^2, m_t^2\right]$ and try to numerically evaluate it via *LoopTools*, but *LoopTools* would fail to evaluate it since the integral is still reducible.

The solution is to use integration-by-parts (IBP) relations, which help to reduce the number of integrals by expressing them through a smaller group of master integrals (MIs). The first automated approach to IBP reduction was introduced by the Laporta algorithm [47] , widely used in various software tools. In this thesis, the *Mathematica* package *LiteRed* [48, 49] was employed to handle the reduction process by identifying symbolic patterns that allow to rewrite all scalar integrals in terms of MIs. A general outline of the method is provided here, more details cand be found in Ref. [50].

Even if this work does not contain any multi-loop calculation, here we will present the IBP method directly.

Following the notation of *LiteRed*, the most general $L$-Loop integral in $D$-dimensions can be written as:

$$j(n_1, n_2, ..., n_N) = \int \frac{\prod_{i=1}^L d^D k_i}{\prod_{j=1}^N D_i^{n_i}}, \tag{5.32}$$

where $k_i$ are the loop momenta and $D_i^{n_i}$ can be either propagators (in which case they can only be raised to a non-negative integer), or scalar products between loop and external momenta (in which case they can be raised to a non-positive integer). If the latter cannot be expressed in terms of the denominators, then they are called irreducible numerators. A set of linearly independent $D_i$ that fall into these categories is called a basis of denominators.

After fixing a basis, one can use a property of scalar integrals in dimensional regularization:

$$\int \prod_{i=1}^L d^D k_i \frac{\partial q_i^\mu}{\partial k_j^\mu} \frac{1}{\prod_{j=1}^N D_i^{n_i}} = 0, \tag{5.33}$$

where the $q_i^\mu$ can either be loop or external momenta. In particular, after differentiating in Eq. (5.33), the scalar products $k_i \cdot q_j$ can be expressed as superposition of the $D_i$, so that the left-hand side of Eq. (5.33) results in an integral in the form of Eq. (5.32), but with different arguments $n_i$.

Therefore, the relations in Eq. (5.33) can be used to recursively express the general integrals

$J(n_1, ..., n_N)$ in terms of a few linearly independent integrals with the same structure but with minimal $n_i$, which constitutes a basis of MIs.

The latter is always finite, even though it is not unique in general.

In the case of the process studied in this thesis, the form factors are not yet in the form of Eq. (5.32), but they can be manipulated with similar tricks as in Eq (4.39) to put them into the right form. In this thesis we used the *FeynCalc* built-in function TID to achieve this. In truth, the output of TID will be in general written in terms of scalar integrals with irreducible numerators $k \cdot r_{3,\perp}$ and $k \cdot r_{4,\perp}$, and denominators belonging to an overdetermined basis. In order to arrive to a true denominator basis, we have to manipulate the integrals manually, which was done with privately written codes.

In the end, we identified two families of denominators that make two basis, so we will have two independent classes of integrals in the form of Eq. (5.32):

$$j_1(n_1, n_2, n_3, n_4, n_5) = \int d^D k \frac{(k \cdot r_{3,\perp})^{n_4} (k \cdot r_{4,\perp})^{n_5}}{[k^2 - m_t^2]^{n_1} [(k+p_1)^2 - m_t^2]^{n_2} [(k-p_2)^2 - m_t^2]^{n_3}}, \qquad (5.34)$$

$$j_2(n_1, n_2, n_3, n_4, n_5) = \int d^D k \frac{(k \cdot r_{3,\perp})^{n_4} (k \cdot r_{4,\perp})^{n_5}}{[k^2 - m_t^2]^{n_1} [(k-p_1)^2 - m_t^2]^{n_2} [(k-p_2)^2 - m_t^2]^{n_3}}. \qquad (5.35)$$

Using *LiteRed* to analyze the two bases, five MIs were identified and the rules used for the IBP reduction were obtained. One additional important feature of the *LiteRed* package used in this work is the function AnalyzeSector, which also allows to search only for MIs without the irreducible numerators, namely with $n_4 = n_5 = 0$. This means that, after the $p_t$ expansion, every integral will only depend on the ratio $\hat{s}/m_t^2$ as desired.

The MIs found by *LiteRed* were the following:

$$j_1(0, 0, 1, 0, 0) = \int d^D k \frac{1}{[(k-p_2)^2 - m_t^2]} \overset{k \to k+p_2}{=} \int d^D k \frac{1}{[k^2 - m_t^2]}, \qquad (5.36)$$

$$j_1(0, 1, 1, 0, 0) = \int d^D k \frac{1}{[(k+p_1)^2 - m_t^2] [(k-p_2)^2 - m_t^2]} \qquad (5.37)$$

$$\overset{k \to k+p_2}{=} \int d^D k \frac{1}{[k^2 - m_t^2] [(k+p_1+p_2)^2 - m_t^2]},$$

$$j_1(1, 1, 1, 0, 0) = \int d^D k \frac{1}{[k^2 - m_t^2] [(k+p_1)^2 - m_t^2] [(k-p_2)^2 - m_t^2]}, \qquad (5.38)$$

$$j_2(0, 1, 1, 0, 0) = \int d^D k \frac{1}{[(k+p_1)^2 - m_t^2] [(k-p_2)^2 - m_t^2]} \qquad (5.39)$$

$$\overset{k \to k+p_2}{=} \int d^D k \frac{1}{[k^2 - m_t^2] [(k+p_1+p_2)^2 - m_t^2]},$$

$$j_2(1, 1, 1, 0, 0) = \int d^D k \frac{1}{[k^2 - m_t^2] [(k-p_1)^2 - m_t^2] [(k-p_2)^2 - m_t^2]}. \qquad (5.40)$$

Since we want to evaluate them numerically using *LoopTools*, it is convenient to show their expression in the PV notation written above, so up to normalization factors, the MIs are:

$$j_1(0, 0, 1, 0, 0) \longrightarrow A_0[m_t^2], \qquad (5.41)$$

$$j_1(0, 1, 1, 0, 0) \longrightarrow B_0[(p_1+p_2)^2, m_t^2, m_t^2], \qquad (5.42)$$

$$j_1(0, 1, 1, 1, 0) \longrightarrow C_0[p_1^2, p_2^2, (p_1 + p_2)^2, m_t^2, m_t^2, m_t^2], \tag{5.43}$$

$$j_2(0, 1, 1, 0, 0) \longrightarrow B_0[(p_1 - p_2)^2, m_t^2, m_t^2], \tag{5.44}$$

$$j_2(0, 1, 1, 1, 0) \longrightarrow C_0[p_1^2, p_2^2(p_1 - p_2)^2, m_t^2, m_t^2, m_t^2]. \tag{5.45}$$

We note the peculiar feature of this expansion: the result depends on integrals with $(p_1+p_2)^2 = \hat{s}$ and $(p_1 - p_2)^2 = -\hat{s}$, so on the scalar integral taken in the Euclidean and Minkowski region. Effectively, we have hence reduced everything to three MIs taken though in the Minkowski and Euclidean regions, the latter being simpler as no branch cuts need to be considered.

## 5.3 Results

In this section we will present the results of the $p_t$ expansions. In order to understand the power of the expansion, we will confront it with the Heavy Top Limit (HTL).

Its primitive version works simply by taking the limit $m_t \to \infty$ before calculating the loop integral. We calculated the expanded form factor on our own up to order $\mathcal{O}\left(\frac{1}{m_t^6}\right)$.

The propagators in the loop functions with loop momentum $k$ can be expanded for small external momentum $p$ and large top mass $m_t$ as:

$$\frac{1}{(k + p)^2 - m_t^2} = \frac{1}{k^2 - m_t^2} \frac{1}{\frac{p^2 + 2k \cdot p}{k^2 - m_t^2}} \simeq \frac{1}{k^2 - m_t^2} - \frac{p^2 + 2k \cdot p}{(k^2 - m_t^2)^2} + ..., \tag{5.46}$$

The expanded results holds for:

$$\frac{\sqrt{\hat{s}}}{2m_t} \ll 1. \tag{5.47}$$

However, this limit is not physical since we need more partonic CoM energy to produce three on-shell Higgs, $\sqrt{\hat{s}} \geq 3m_H$ as was explained in in Section 3.3, so we already expect the result to diverge for very moderate partonic CoM energies.

We present now the results of the $p_t$ expansion.

We calculated only the first form factor since it is the one that gives by far the largest contribution as we saw in Fig. 4.4.

We are missing only the small yet non-negligible contribution from the second form factor, but the algorithm presented in this thesis can very easily be adapted to calculate it.
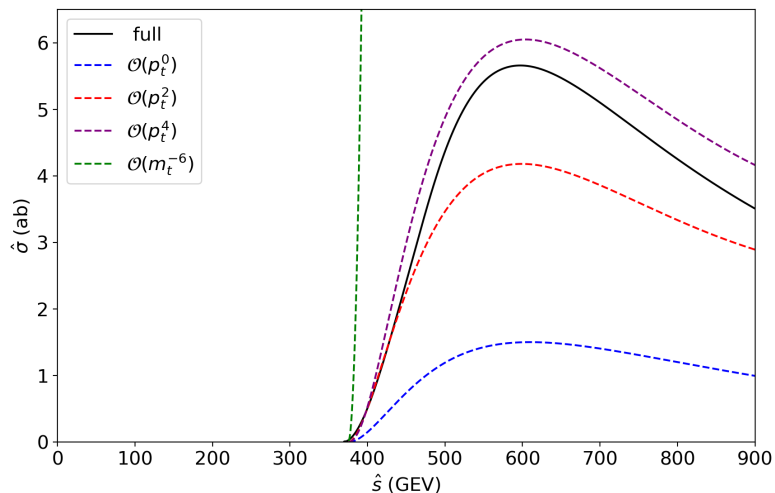


Figure 5.2: Pentagon contributions to the cross section, only relative to the first form factor.

In Fig. 5.2, we can see the contributions to the cross section coming from the pentagon topologies of the first firm factor. The full line represents the full (not expanded) cross section, whereas the dotted lines represent the expanded cross section at different orders in the $p_t$ expansion and in the HTL.

As expected, the HTL does not work at all in reproducing the Triple Higgs production cross section.

On the other hand, the $p_t$ expansion gets better as we include higher orders. We had to stop at the second order because using the limiting computational power of a desktop computer did not allow to go beyond.

This is the biggest practical limitation of this technique: the symbolic computations needed to simplify the form factors extensively slows down the algorithm. The intermediate expression for the second-order expansion term had a size in the $\mathcal{O}(20)$ GB and typically each term increased with a factor $\sim 100$ with respect to the previous one in the Taylor expansion.

Another factor why the expansion does not overlap completely with the full result might be inherit at the approximations made. Here we had the goal to reduce the number of scales to one, but a better approximation might be to combine various expansions or in alternative keep some kinematic variables as arbitrarily large. The approach presented in this thesis was though to investigate whether it will be really possible to reduce the amount of scales completely to one to allow for relatively simple Master integrals when applying this method an order higher in perturbation theory. We can conclude, that the proposed method will surely lead to more accurate results than the infinite top mass limit employed so far for the computation of higher order corrections to triple Higgs production [14]

# Chapter 6

# Conclusions

Precise theoretical predictions are needed in order to compare with the increasingly precise experimental measurements.

The QCD corrections to gluon-initiated processes are expected to be substantial, but the calculation of two-loop multi-scale integrals related to 2→3 processes are currently beyond the state-of-the-art.

In this thesis, we calculated the Leading Order contribution to the cross section of Triple Higgs Production via gluon fusion at the LHC. Afterwards, we extended the method of $p_t$ expansion from Ref. [15, 17] for the first time to a case of $2 \to 3$ kinematics.

In chapter 3 we discussed how we numerically calculated the multi-dimensional integral needed for the cross section of a 2→3 process at hadronic colliders.

We implemented our own 3-particle phase space [28] using a Monte Carlo integration routine known as VEGAS [29], with implementation of the CUBA library [30]. This implementation could be cross-checked numerically with RAMBO [31].

In chapter 4 we discussed the method to calculate the full LO cross section of $gg \to HHH$. The LO contribution is generated at the one-loop level and the Feynman diagrams (Fig. 4.1) are composed of triangle, box, and pentagon topologies with a quark running in the loop. Since the Higgs coupling is proportional to the mass of the particle it couples to, the process is dominated by the top quark loops and approximate the masses of all the quarks to zero. We checked *a posteriori* that their contribution is negligible: already the bottom quark gave corrections inside the VEGAS integration error.

The tensorial amplitude was decomposed along an orthonormal basis of four independent projectors, exploiting all the symmetries of the problems, each multiplied by its scalar form factor. The form factors were then calculated with the help of *Mathematica* packages, like *FeynArts* [32], and *FeynCalc* [36]. In particular, the loop integrals were reduced using the Passarino-Veltmann method [40], so that the form factors would only depend on the masses of the particles in the Feynman diagrams ($m_H$ and $m_t$), on the five independent kinematic variables ($\hat{s}$, $\hat{s}_1$, $\hat{s}_2$, $\hat{t}_1$, $\hat{t}_2$) and on the four independent PV scalar functions (Eqs. (4.26)-(4.29)).

The form factors were then translated to FORTRAN language using *FormCalc* [45], and written in separate subroutines, keeping separated also the contributions from different topologies to each form factor and the numerical evaluation of the PV functions was done using *Loop-Tools* [43].

The hadronic cross section was calculated for different CoM energies of the incoming protons at LHC. The result for the current accessible CoM energy ($\sqrt{s} = 14$ TeV) is $\sigma = 24.88 \pm 0.05$

ab, where the uncertainty is given simply as the integration error of the VEGAS routine.
The result is compatible with the one in Ref. [14] within uncertainties and up to the change of
the input parameters.


In chapter 5 we discussed the implementation of the $p_t$ expansion for this process.
The expansion of the box integrals could be related to the work on Double Higgs production in
Ref. [15], since the amplitude has a very similar structure but with one of the two Higgs being
off-shell.
The expansion of the pentagon diagrams, instead, was conducted here for the first time.
The momenta of the final state were decomposed into two parts: one parallel to the beam axis,
and one perpendicular to it. To do so, two space-like four momenta were identified ($r_{3,\perp}$ and
$r_{4,\perp}$), and their squares were precisely the inverse of the square of the transverse momenta of
the Higgs particles, see Eq. (5.9).
The form factors were then expressed only in terms of the quantities in Eq. (5.15) and the
top mass. A subset of these quantities, namely the small parameters to be expended in, were
rescaled by a common scale $x$, and the form factors were Taylor-expanded around $x = 0$ at the
integrand level.
The Tensor Integral Decomposition [41] was conducted again with *FeynCalc*, but the integrals
were not independent yet, so we used Integration By Parts relations to express the form factors
only in terms of 5 Master Integrals. The IBP reduction was conducted using *LiteRed* [49].
At the end, we used the same integration technique to get the approximated partonic cross
section at different orders of the $p_t$ expansion.
We saw that a second order approximation already is in agreement with the exact result in the
phase space region where they give the largest contribution to the cross section.


Implementing the $p_t$ expansion on the calculation of the cross section of Triple Higgs Produc-
tion gave some insight about some limitations that it brings.
The great advantage of the $p_t$ expansion is the computation time needed to do the Montecarlo
integration to get the cross section. In fact, it drops down significantly and this will be true
in particular for NLO calculations. The reason is that the expanded form factors have a really
simple expression where the scalar MIs depend only on one energy scale, as previously men-
tioned.
However, the expansion of the form factors takes a lot of computation power; In particular,
what took the longest was the symbolic simplifications after the Tensor Integral Decomposition
and after the IBP reduction.
Each higher order of the expansion increased the space occupied by the intermediate expression
by a factor of roughly 100. This has forced us to stop the expansion at $\mathcal{O}(p_t^2)$. However, the
results are very promising, given the high number of approximations.
It is also true that the optimized usage of *Mathematica*, alongside its computing resources and
satellite packages, made it possible for us to develop this expansion on a desktop computer. One
should also note, that while for the computation of the analytic result at LO, the intermediate
expressions occupy a large space, an analytic computation of the full NLO QCD corrections for
the process is currently beyond the state of the art.


Even though the expansion works only in a region of the phasespace (the more enhanced by the
PDFs at the current CoM energies), in the future one could also think to find approximations
to recover the behaviour at high energies in order to merge the two like it was done with a
varity of top-quark mediated 2→2 processes [15–17, 46].
As a final remark, we note that this might represent only the beginning of the implementation

of transverse momentum expansions in the context of top-quark mediated 2→3 processes. The power of these kinds of approximations is process-dependent, but we found an algorithm that could be adapted in principle to the prediction of other processes, such as $gg \to HHg$, which would be crucial as it is responsible for the cancelation of IR divergences in the NLO QCD corrections of Double-Higgs production, which has a much higher cross section.

# Appendix A

## A.1

- The integration limits of $\hat{s}_1$ are the following:

$$\hat{s}_1^{\max} = \frac{m_H^4(\hat{s}_2 - \hat{t}_1) + m_H^2(\hat{s}(\hat{s}_2 + \hat{t}_1) - (\hat{s}_2 - \hat{t}_1)(\hat{t}_1 + \hat{t}_2)) - \hat{s}\hat{s}_2\hat{t}_1 - \hat{s}\hat{s}_2\hat{t}_2 + \hat{s}\hat{t}_1^2}{(\hat{s}_2 - \hat{t}_1)^2} \quad \text{(A.1)}$$

$$+ \frac{\hat{s}_2^2\hat{t}_2 - \hat{s}\hat{t}_1\hat{t}_2 - \hat{s}_2\hat{t}_1\hat{t}_2 + 2\sqrt{\eta}}{(\hat{s}_2 - \hat{t}_1)^2},$$

$$\hat{s}_1^{\min} = \frac{m_H^4(\hat{s}_2 - \hat{t}_1) + m_H^2(\hat{s}(\hat{s}_2 + \hat{t}_1) - (\hat{s}_2 - \hat{t}_1)(\hat{t}_1 + \hat{t}_2)) - \hat{s}\hat{s}_2\hat{t}_1 - \hat{s}\hat{s}_2\hat{t}_2 + \hat{s}\hat{t}_1^2}{(\hat{s}_2 - \hat{t}_1)^2} \quad \text{(A.2)}$$

$$+ \frac{\hat{s}_2^2\hat{t}_2 - \hat{s}\hat{t}_1\hat{t}_2 - \hat{s}_2\hat{t}_1\hat{t}_2 - 2\sqrt{\eta}}{(\hat{s}_2 - \hat{t}_1)^2},$$

where

$$\eta = \hat{s}(m_H^2(\hat{s}_2 - \hat{t}_1) + \hat{t}_1(\hat{s} - \hat{s}_2 + \hat{t}_1))(m_H^4\hat{s}_2 + m_H^2(\hat{t}_1^2 - \hat{s}_2(\hat{t}_1 + 2\hat{t}_2)) + \hat{s}_2\hat{t}_2(\hat{s}_2 - \hat{t}_1 + \hat{t}_2)). \quad \text{(A.3)}$$

- The Jacobian of the transformation from $\varphi \to \hat{s}_1$ is the following:

$$J_1 = \sqrt{-\frac{(\hat{s}_2 - \hat{t}_1)^2}{m_H^8 + c_6 m_H^6 + c_4 m_H^4 + c_2 m_H^2 + c_0}}, \quad \text{(A.4)}$$

where

$$c_6 = -2(\hat{s} + \hat{t}_1 + \hat{t}_2), \quad \text{(A.5)}$$

$$c_4 = (\hat{s}^2 + 4\hat{s}(\hat{t}_1 + \hat{t}_2) + 2\hat{s}_1(\hat{t}_1 - \hat{s}_2) + 2\hat{s}_2\hat{t}_2 + (\hat{t}_1 + \hat{t}_2)^2 \quad \text{(A.6)}$$

$$c_2 = -2(\hat{s}^2(\hat{t}_1 + \hat{t}_2) + \hat{s}(\hat{s}_1(\hat{s}_2 + \hat{t}_1) + \hat{t}_2(\hat{s}_2 + \hat{t}_2) + \hat{t}_1^2) + (\hat{t}_1 + \hat{t}_2)(\hat{s}_1(\hat{t}_1 - \hat{s}_2) + \hat{s}_2\hat{t}_2)), \quad \text{(A.7)}$$

$$c_0 = 2\hat{s}_1(\hat{s}\hat{t}_2(\hat{s}_2 + \hat{t}_1) + \hat{s}\hat{t}_1(\hat{s}_2 - \hat{t}_1) + \hat{s}_2\hat{t}_2(\hat{t}_1 - \hat{s}_2)) + (\hat{s}(\hat{t}_1 - \hat{t}_2) + \hat{s}_2\hat{t}_2)^2 + \hat{s}_1^2(\hat{s}_2 - \hat{t}_1)^2. \quad \text{(A.8)}$$

## A.2

The third and fourth projectors are the following:

$$\hat{\mathcal{S}}_3^{\mu\nu} = \frac{(p_3^\mu(p_1 \cdot p_2) - p_2^\mu(p_1 \cdot p_3))}{(p_3^2(p_1 \cdot p_2) - 2(p_1 \cdot p_3)(p_2 \cdot p_3))(p_1 \cdot p_2)^2} \tag{A.9}$$

$$\times (p_1^\nu(-(p_1 \cdot p_4)(p_2 \cdot p_3)^2 + (p_1 \cdot p_3)(p_2 \cdot p_3)(p_2 \cdot p_4) + (p_1 \cdot p_2)((p_2 \cdot p_3)(p_3 \cdot p_4) - p_3^2(p_2 \cdot p_4)))$$

$$+ p_4^\nu(p_1 \cdot p_2)(p_3^2(p_1 \cdot p_2) - 2(p_1 \cdot p_3)(p_2 \cdot p_3)) + p_3^\nu(p_1 \cdot p_2)((p_1 \cdot p_4)(p_2 \cdot p_3) + (p_1 \cdot p_3)(p_2 \cdot p_4) - (p_1 \cdot p_2)(p_3 \cdot p_4)))$$

$$\hat{\mathcal{S}}_4^{\mu\nu} = \frac{(p_3^\mu(p_1 \cdot p_2) - p_1^\mu(p_2 \cdot p_3))}{(p_3^2(p_1 \cdot p_2) - 2(p_1 \cdot p_3)(p_2 \cdot p_3))(p_1 \cdot p_2)^2} \tag{A.10}$$

$$\times (p_2^\nu(-(p_2 \cdot p_4)(p_1 \cdot p_3)^2 + (p_1 \cdot p_3)((p_1 \cdot p_4)(p_2 \cdot p_3) + (p_1 \cdot p_2)(p_3 \cdot p_4)) - p_3^2(p_1 \cdot p_2)(p_1 \cdot p_4))$$

$$+ p_4^\nu(p_1 \cdot p_2)(p_3^2(p_1 \cdot p_2) - 2(p_1 \cdot p_3)(p_2 \cdot p_3)) + p_3^\nu(p_1 \cdot p_2)((p_1 \cdot p_4)(p_2 \cdot p_3) + (p_1 \cdot p_3)(p_2 \cdot p_4) - (p_1 \cdot p_2)(p_3 \cdot p_4)))$$

# Appendix B

## B.1

We report the FORTRAN code used to calculate the hadronic cross section

```fortran
 program CubaTest
 implicit none
#include "/Library/Mathematica/Applications/LoopTools-2.16/x86_64-Darwin/include/looptoo
 CHARACTER*30 PDFNAME, PATHNAME
 integer ndim, ncomp, nvec, last, seed, mineval, maxeval
 double precision epsrel, epsabs, userdata
 parameter (ndim = 6)
 parameter (ncomp = 1)
 parameter (userdata = 0)
 parameter (nvec = 1)
 parameter (epsrel = 1D-3)
 parameter (epsabs = 1D-12)
 parameter (last = 4)
 parameter (seed = 0)
 parameter (mineval = 0)
 parameter (maxeval = 50000)

 integer res,vega,value
 parameter(res=98,vega=99,value=97)

 integer nstart, nincrease, nbatch, gridno
 integer*8 spin
 character*(*) statefile
 parameter (nstart = 1000)
 parameter (nincrease = 500)
 parameter (nbatch = 1000)
 parameter (gridno = 0)
 parameter (statefile = "")
 parameter (spin = -1)

 integer nnew, nmin
```

```
double precision flatness
parameter (nnew = 1000)
parameter (nmin = 2)
parameter (flatness = 25D0)

integer key1, key2, key3, maxpass
double precision border, maxchisq, mindeviation
integer ngiven, ldxgiven, nextra
parameter (key1 = 47)
parameter (key2 = 1)
parameter (key3 = 1)
parameter (maxpass = 5)
parameter (border = 0D0)
parameter (maxchisq = 10D0)
parameter (mindeviation = .25D0)
parameter (ngiven = 0)
parameter (ldxgiven = ndim)
parameter (nextra = 0)

integer key
parameter (key = 0)

external integrand


double precision integral(ncomp), error(ncomp), prob(ncomp)
integer verbose, nregions, neval, fail
character*16 env

integer c

integer LOOP,N0
double precision AMZ,AMH,mh,mw,v,gf,sinw,amb,xitla,amq
double precision amb2,amc,ALSMZ,amt,AMW,XLAMBDA,ecms
common/input/ECMS, AMZ, AMH, AMQ, v, amb2, SINW
COMMON/ALS/XLAMBDA,AMC,AMB,AMT,N0
parameter (mh=125.d0)
parameter (gf=1.16639d-5)
parameter (mw=80.423d0)

PDFNAME="NNPDF40_lo_as_01180"

CALL PDFSET(PATHNAME,PDFNAME)


AMZ=91.1874d0
AMH= mh
AMW=mw
LOOP=1
v=1.d0/dsqrt(dsqrt(2.d0)*gf)
```

```
 sinw=dsqrt(1d0-amw**2/amz**2)
 amb=4.62d0
 AMB2=AMB**2
 amc=1.42d0
 ALSMZ=0.118d0
 NO=5
 LOOP=1
 amt=173.3d10
 XLAMBDA=XITLA(LOOP,ALSMZ,1d-8)


 CALL ALSINI(1d-8)

 call getenv("CUBAVERBOSE", env)
 verbose = 2
 read(env, *, iostat=fail, end=999, err=999) verbose
999 continue

 print *, "------------------- Vegas test -------------------"

 call vegas(ndim, ncomp, integrand, userdata, nvec,
     &      epsrel, epsabs, verbose, seed,
     &      mineval, maxeval, nstart, nincrease, nbatch,
     &      gridno, statefile, spin,
     &      neval, fail, integral, error, prob)

 print *, "neval    =", neval
 print *, "fail     =", fail
 print '(F20.12," +- ",F20.12,"   p = ",F8.3)',
     &      (integral(c), error(c), prob(c), c = 1, ncomp)
c other integration rouutines in the following, not used
 print *, " "
c print *, "------------------- Suave test -------------------"
c
c call suave(ndim, ncomp, integrand, userdata, nvec,
c     &      epsrel, epsabs, verbose + last, seed,
c     &      mineval, maxeval, nnew, nmin, flatness,
c     &      statefile, spin,
c     &      nregions, neval, fail, integral, error, prob)
c
c print *, "nregions =", nregions
c print *, "neval    =", neval
c print *, "fail     =", fail
c print '(F20.12," +- ",F20.12,"   p = ",F8.3)',
c     &      (integral(c), error(c), prob(c), c = 1, ncomp)
c
c print *, " "
c print *, "------------------- Divonne test ------------------"

c call divonne(ndim, ncomp, integrand, userdata, nvec,
```

```
c     &      epsrel, epsabs, verbose, seed,
c     &      mineval, maxeval, key1, key2, key3, maxpass,
c     &      border, maxchisq, mindeviation,
c     &      ngiven, ldxgiven, 0, nextra, 0,
c     &      statefile, spin,
c     &      nregions, neval, fail, integral, error, prob)

c print *, "nregions =", nregions
c print *, "neval    =", neval
c print *, "fail     =", fail
c print '(F20.12," +- ",F20.12,"   p = ",F8.3)',
c     &      (integral(c), error(c), prob(c), c = 1, ncomp)

c print *, " "
c print *, "------------------- Cuhre test -------------------"

c call cuhre(ndim, ncomp, integrand, userdata, nvec,
c     &      epsrel, epsabs, verbose + last,
c     &      mineval, maxeval, key,
c     &      statefile, spin,
c     &      nregions, neval, fail, integral, error, prob)

c print *, "nregions =", nregions
c print *, "neval    =", neval
c print *, "fail     =", fail
c print '(F20.12," +- ",F20.12,"   p = ",F8.3)',
c     &      (integral(c), error(c), prob(c), c = 1, ncomp)
  end


************************************************************************
c This is the integrand
 integer function integrand(ndim, xx, ncomp, ff)
 implicit none
 integer ndim, ncomp
 double precision xx(*), ff(*)

#define f ff(1)

 double precision g3h,g4h,mh,g,mt,mw,gf
 double precision pi,ecms,s,s1,s2,t1,t2
 double precision s1max,s1min,jac,up1
 double precision s2min,s2max,t1min,t1max,t2min,t2max
 double precision lambda1,lambda2,factors1
 double precision q,alphs,gs,alphas
 double precision norm1,norm2,norm3,norm4
 double precision Ampli,norm,intfactor,intphase
 double precision invmass,tau1,tau,ecmstot,x2m,x2p,x2,scala
 double precision lum,fp1(-6:6),fp2(-6:6)
 complex*16 ampt1,ampb1,ampb2,ampb3,ampb4
```

```
      complex*16 ampp1,ampp2,ampp3,ampp4
      complex*16 ampb3n,ampb4n,ampp3n,ampp4n
      parameter (pi = 4.D0*datan(1.D0))
      parameter (ecmstot=14000.d0)
c parameter (ecms=14000.d0)
c parameter (s=ecms**2.d0)
      parameter (mh=125.0d0)
      parameter (gf=1.16639d-5)
      parameter (mt=173.3d0)
      parameter (mw=80.423d0)
      parameter (g4h=6.d0*mh**2.d0*gf/dsqrt(2.d0))
      parameter (g3h=3.d0*mh**2.d0*dsqrt(2.d0)*dsqrt(gf/dsqrt(2.d0)))
      parameter (g=dsqrt(8.d0*mw**2.d0*gf/dsqrt(2.d0)))
      parameter (norm=0.3894D15)

      invmass= (3.d0*mh)**2.d0
      tau1=invmass/(ecmstot**2.d0)
      tau=tau1**xx(1)
c --- the x2 integration ---------

      s=tau*ecmstot**2.d0
      x2m = tau
      x2p = 1.D0
c--- phase mapping

      x2=tau1**(xx(1)*xx(2))

c --- the scala --------

      scala = 0.5d0*dsqrt(s)

      call struc(x2,scala,fp1)
      call struc(tau/x2,scala,fp2)

c ---luminosity
      lum=dlog(tau1)*dlog(tau)*fp1(0)*fp2(0)
      ecms=dsqrt(s)




      s2min=(2.d0*mh)**2.d0
      s2max=(ecms-mh)**2.d0
      s2=(s2max-s2min)*xx(3)+s2min

      lambda1=(s+mh**2.d0-s2)**2.d0-4.d0*mh**2.d0*s
      lambda2=s2**2.d0-4.d0*mh**2.d0*s2

      t1max=1.d0/2.d0*(s+mh**2.d0-s2+dsqrt(lambda1))
```

```
t1min=1.d0/2.d0*(s+mh**2.d0-s2-dsqrt(lambda1))
t1=(t1max-t1min)*xx(4)+t1min


t2max=(s2+t1-mh**2.d0)/(s2)*(1.d0/2.d0)*(s2+dsqrt(lambda2))
t2min=(s2+t1-mh**2.d0)/(s2)*(1.d0/2.d0)*(s2-dsqrt(lambda2))
t2=(t2max-t2min)*xx(5)+t2min


s1max = (t2*(s2**2.D0+(s+s2)*t1-1.D0*(s*s2))+
    &t1*(s*s2-2.D0*s2**2.D0)-mh**4.D0*(-t2+5.D0*s2+4.D0*t1)-
    &1.D0*(s2**3.D0+s2*t1**2.D0)+
    &mh**2.D0*(t1+2.D0*s2)*(2.D0*(s2+t1)-1.D0*t2)+
    &s*(s2**2.D0-1.D0*(mh**2.D0*(s2+t2)))+
    &2.D0*(mh**6.D0+dsqrt(s*
    &(t1*(s2+t1-1.D0*mh**2.D0)+s*(mh**2.D0-1.D0*t1))*
    &(mh**6.D0+
    &mh**2.D0*(s2**2.D0+t1**2.D0+s2*(t2+2.D0*t1))-
    &2.D0*(mh**4.D0*(s2+t1))-
    &1.D0*(s2*t2*(s2+t1-1.D0*t2))))))/
    &(1.D0*mh**2.D0-1.D0*(s2+t1))**2.d0


s1min = (2.D0*mh**6.D0+
    &t2*(s2**2.D0+(s+s2)*t1-1.D0*(s*s2))+
    &t1*(s*s2-2.D0*s2**2.D0)-mh**4.D0*(-t2+5.D0*s2+4.D0*t1)-
    &1.D0*(s2**3.D0+s2*t1**2.D0)+
    &mh**2.D0*(t1+2.D0*s2)*(2.D0*(s2+t1)-1.D0*t2)+
    &s*(s2**2.D0-1.D0*(mh**2.D0*(s2+t2)))-
    &2.D0*dsqrt(s*(t1*(s2+t1-1.D0*mh**2.D0)+
    &s*(mh**2.D0-1.D0*t1))*
    &(mh**6.D0+mh**2.D0*
    &(s2**2.D0+t1**2.D0+s2*(t2+2.D0*t1))-
    &2.D0*(mh**4.D0*(s2+t1))-
    &1.D0*(s2*t2*(s2+t1-1.D0*t2)))))/
    &(1.D0*mh**2.D0-1.D0*(s2+t1))**2.d0
      s1=(s1max-s1min)*xx(6)+s1min
c jacobian phi->s1


up1 = s1+3.D0*s2+2.D0*t1-1.D0*t2

jac = dsqrt(1.D0*(-(1.D0*mh**2.D0)+1.D0*(s2+t1))**2.D0/
    &(4.D0*(up1*mh**6.D0)-4.D0*mh**8-
    &t2**2.D0*(s-1.D0*s2)**2.D0-
    &(-(1.D0*(s1*t1))+s2*(s-1.D0*(s1+s2+t1)))**2.D0+
    &mh**4.D0*(-s1**2.D0-t2**2.D0+4.D0*s**2.D0+
    &t1*(-(8.D0*s1)-16.D0*s2)-10.D0*(s1*s2)-
    &13.D0*s2**2.D0-4.D0*t1**2.D0+
    &4.D0*(s*(s2+t2-1.D0*t1))+
    &2.D0*(t2*(s1+5.D0*s2+2.D0*t1)))+
    &2.D0*(t2*(s2*(s1+s2)*(s2+t1)+s*t1*(s1-1.D0*s2)+
    &s2*(s**2.D0-1.D0*(s*(s1+2.D0*s2)))))-
```

```
      &2.D0*(mh**2.D0*(2.D0*(s**2.D0*t1)+
      &s*(s2*(s1+3.D0*s2)+t2*(s1-2.D0*s2+2.D0*t1)-
      &2.D0*t1**2.D0-1.D0*t2**2.D0)-
      &1.D0*(up1*(s1*(s2+t1)+s2*(s2+t1-1.D0*t2))))
      &)))

 q=0.5d0*DSQRT(S)
 alphs=alphas(q,1)
 gs=dSqrt(alphs*4.d0*pi)
c Here I call the subroutines (from a different file .F) where I stored the topology con
 call triangle(ampt1,g,gs,mt,s,g4h,s1,s2,g3h,mh,pi,mw)
 call box1(ampb1,g,gs,mt,s,s1,s2,mh,pi,mw,t1,t2)
 call box2(ampb2,g,gs,mt,s,s1,s2,mh,pi,mw,t1,t2)
 call box3(ampb3,g,gs,mt,s,s1,s2,mh,pi,mw,t1,t2)
 call box4(ampb4,g,gs,mt,s,s1,s2,mh,pi,mw,t1,t2)
 call pent1(ampp1,g,gs,mt,s,s1,s2,mh,pi,mw,t1,t2)
 call pent2(ampp2,g,gs,mt,s,s1,s2,mh,pi,mw,t1,t2)
 call pent3(ampp3,g,gs,mt,s,s1,s2,mh,pi,mw,t1,t2)
 call pent4(ampp4,g,gs,mt,s,s1,s2,mh,pi,mw,t1,t2)

 norm1=2.d0

 norm2=2.d0

 norm3=0.25D0*(4.D0*((s1+3.D0*s2+2.D0*t1-1.D0*t2)
      &*mh**6.D0)-4.D0*mh**8.D0+
      &mh**4.D0*(t1*(-(8.D0*s1)-16.D0*s2)-10.D0*(s1*s2)-
      &13.D0*s2**2.D0-4.D0*t1**2.D0-1.D0*(s1**2.D0+t2**2.D0)+
      &4.D0*(s**2.D0+s*(s2+t2-1.D0*t1))+
      &2.D0*(t2*(s1+5.D0*s2+2.D0*t1)))-
      &1.D0*(t2**2.D0*(s-1.D0*s2)**2.D0+
      &(-(1.D0*(s1*t1))+s2*(s-1.D0*(s1+s2+t1)))**2.D0)+
      &2.D0*(t2*(s*t1*(s1-1.D0*s2)+
      &s2*(s**2.D0+(s1+s2)*(s2+t1)-
      &1.D0*(s*(s1+2.D0*s2)))))-
      &2.D0*(mh**2.D0*(2.D0*(s**2.D0*t1)-
      &(s1+3.D0*s2+2.D0*t1-1.D0*t2)*(s1*(s2+t1)+s2*(s2+t1-1.D0*t2))+
      &s*(-t2**2.D0-2.D0*t1**2.D0+
      &1.D0*(s2*(s1+3.D0*s2)+t2*(s1-2.D0*s2+2.D0*t1))
      &)))))/s**2

 norm4 = norm3


 ampt1=ampt1/norm1
 ampb1=ampb1/norm1*g3h
 ampp1=ampp1/norm1

 ampb2=ampb2/norm2*g3h
 ampp2=ampp2/norm2
```

```
ampb3n=ampb3*g3h/norm3
ampp3n=ampp3/norm3


ampb4n=ampb4*g3h/norm4
ampp4n=ampp4/norm4



Ampli=
     & ampt1*Conjg(ampt1)
     & +ampt1*Conjg(ampb1)
     & +ampb1*Conjg(ampt1)
     & +ampb1*Conjg(ampb1)
     & +ampt1*Conjg(ampp1)
     & +ampp1*Conjg(ampt1)
     & +ampb1*Conjg(ampp1)
     & +ampp1*Conjg(ampp1)
     & +ampp1*Conjg(ampb1)
     & +ampb2*Conjg(ampb2)
     & +ampb2*Conjg(ampp2)
     & +ampp2*Conjg(ampb2)
     & +ampp2*Conjg(ampp2)
     & +ampb3n*Conjg(ampb3n)
     & +ampb3n*Conjg(ampp3n)
     & +ampp3n*Conjg(ampb3n)
     & +ampp3n*Conjg(ampp3n)
     & +ampb4n*Conjg(ampb4n)
     & +ampb4n*Conjg(ampp4n)
     & +ampp4n*Conjg(ampb4n)
     & +ampp4n*Conjg(ampp4n)

c intfactor is the prefactor before the integral
c      intfactor=1.d0/(49152.d0*pi**4.d0*s**2.d0*(s2+t1-mh**2.d0))
c lum is the integral for the PDF
c norm is to go from GeV^-2 to attobarn
c Ampli is the squared of the form factors
c factors1 is the jacobian for the change of variables to integrate in the hypercube

 factors1=dabs((s2max-s2min)*(t1max-t1min)*
     &    (t2max-t2min)*(s1max-s1min))

 intfactor=1.d0/(49152.d0*pi**4.d0*s**2.d0*(s2+t1-mh**2.d0))

 f=intfactor*factors1*jac*Ampli*norm*lum
```

```
  end




c------ the following routines have been copied from hpair and may be needed in the main
ccccccccccccccccccccccccccccccccccc
 DOUBLE PRECISION FUNCTION ALPHAS(Q,N)
C--ALPHA_S: Q = SCALE, N = 1 -> LO, N = 2 -> NLO
 IMPLICIT DOUBLE PRECISION (A-H,O-Z)
 DIMENSION XLB(6)
 COMMON/ALSLAM/XLB1(6),XLB2(6)
 COMMON/ALS/XLAMBDA,AMC,AMB,AMT,N0
 B0(NF)=33.D0-2.D0*NF
 B1(NF)=6.D0*(153.D0-19.D0*NF)/B0(NF)**2
 ALS1(NF,X)=12.D0*PI/(B0(NF)*DLOG(X**2/XLB(NF)**2))
 ALS2(NF,X)=12.D0*PI/(B0(NF)*DLOG(X**2/XLB(NF)**2))
     .              *(1.D0-B1(NF)*DLOG(DLOG(X**2/XLB(NF)**2))
     .               /DLOG(X**2/XLB(NF)**2))
 PI=4.D0*DATAN(1.D0)


 IF(N.EQ.1)THEN
 DO 1 I=1,6
 XLB(I)=XLB1(I)
1      CONTINUE
 ELSE
 DO 2 I=1,6
 XLB(I)=XLB2(I)
2      CONTINUE
 ENDIF




 IF(Q.LT.AMC)THEN
 NF=3
 ELSEIF(Q.LE.AMB)THEN
 NF=4
 ELSEIF(Q.LE.AMT)THEN
 NF=5
 ELSE
 NF=6
 ENDIF
 IF(N.EQ.1)THEN
 ALPHAS=ALS1(NF,Q)
 ELSE
 ALPHAS=ALS2(NF,Q)
 ENDIF
 RETURN
 END
```

```
 SUBROUTINE ALSINI(ACC)
C--ALPHA_S: INITIALIZATION OF LAMBDA_NF, ACC = ACCURAY AT THRESHOLDS
 IMPLICIT DOUBLE PRECISION (A-H,O-Z)
 DIMENSION XLB(6)
 COMMON/ALSLAM/XLB1(6),XLB2(6)
 COMMON/ALS/XLAMBDA,AMC,AMB,AMT,N0
 B0(NF)=33.D0-2.D0*NF
 B1(NF)=6.D0*(153.D0-19.D0*NF)/B0(NF)**2
 ALS2(NF,X)=12.D0*PI/(B0(NF)*DLOG(X**2/XLB(NF)**2))
     .              *(1.D0-B1(NF)*DLOG(DLOG(X**2/XLB(NF)**2))
     .               /DLOG(X**2/XLB(NF)**2))
 PI=4.D0*DATAN(1.D0)
 XLB1(1)=0D0
 XLB1(2)=0D0
 XLB2(1)=0D0
 XLB2(2)=0D0

 IF(N0.EQ.4)THEN
 XLB(4)=XLAMBDA
 XLB(5)=XLB(4)*(XLB(4)/AMB)**(2.D0/23.D0)
 ELSEIF(N0.EQ.5)THEN
 XLB(5)=XLAMBDA
 XLB(4)=XLB(5)*(XLB(5)/AMB)**(-2.D0/25.D0)
 ENDIF
 XLB(3)=XLB(4)*(XLB(4)/AMC)**(-2.D0/27.D0)
 XLB(6)=XLB(5)*(XLB(5)/AMT)**(2.D0/21.D0)
 DO 1 I=1,6
 XLB1(I)=XLB(I)
1     CONTINUE
 IF(N0.EQ.4)THEN
 XLB(4)=XLAMBDA
 XLB(5)=XLB(4)*(XLB(4)/AMB)**(2.D0/23.D0)
     .              *(2.D0*DLOG(AMB/XLB(4)))**(-963.D0/13225.D0)
 XLB(5)=XITER(AMB,XLB(4),4,XLB(5),5,ACC)
 ELSEIF(N0.EQ.5)THEN
 XLB(5)=XLAMBDA
 XLB(4)=XLB(5)*(XLB(5)/AMB)**(-2.D0/25.D0)
     .              *(2.D0*DLOG(AMB/XLB(5)))**(963.D0/14375.D0)
 XLB(4)=XITER(AMB,XLB(5),5,XLB(4),4,ACC)
 ENDIF
 XLB(3)=XLB(4)*(XLB(4)/AMC)**(-2.D0/27.D0)
     .              *(2.D0*DLOG(AMC/XLB(4)))**(107.D0/2025.D0)
 XLB(3)=XITER(AMC,XLB(4),4,XLB(3),3,ACC)
 XLB(6)=XLB(5)*(XLB(5)/AMT)**(2.D0/21.D0)
     .              *(2.D0*DLOG(AMT/XLB(5)))**(-321.D0/3381.D0)
 XLB(6)=XITER(AMT,XLB(5),5,XLB(6),6,ACC)
 DO 2 I=1,6
 XLB2(I)=XLB(I)
2     CONTINUE
 RETURN
```

```
 END

 DOUBLE PRECISION FUNCTION XITER(Q,XLB1,NF1,XLB,NF2,ACC)
C--ALPHA_S: ITERATION FOR ALPHA_S(M_Z) -> LAMBDA_5
 IMPLICIT DOUBLE PRECISION (A-H,O-Z)
 B0(NF)=33.D0-2.D0*NF
 B1(NF)=6.D0*(153.D0-19.D0*NF)/B0(NF)**2
 ALS2(NF,X,XLB)=12.D0*PI/(B0(NF)*DLOG(X**2/XLB**2))
     .                *(1.D0-B1(NF)*DLOG(DLOG(X**2/XLB**2))
     .                /DLOG(X**2/XLB**2))
 AA(NF)=12D0*PI/B0(NF)
 BB(NF)=B1(NF)/AA(NF)
 XIT(A,B,X)=A/2.D0*(1D0+DSQRT(1D0-4D0*B*DLOG(X)))
 PI=4.D0*DATAN(1.D0)
 XLB2=XLB
 IF(ACC.GE.1.D0) GOTO 111
 II=0
1      II=II+1
 X=DLOG(Q**2/XLB2**2)
 ALP=ALS2(NF1,Q,XLB1)
 A=AA(NF2)/ALP
 B=BB(NF2)*ALP
 XX=XIT(A,B,X)
 XLB2=Q*DEXP(-XX/2.D0)
 Y1=ALS2(NF1,Q,XLB1)
 Y2=ALS2(NF2,Q,XLB2)
 DY=DABS(Y2-Y1)/Y1
 IF(DY.GE.ACC) GOTO 1
111    XITER=XLB2
 RETURN
 END

 DOUBLE PRECISION FUNCTION XITLA(NO,ALP,ACC)
C--ITERATION ROUTINE TO DETERMINE IMPROVED LAMBDAS
 IMPLICIT DOUBLE PRECISION (A-H,O-Z)
 common/input/AECMS, AMZ, AMH, AMQ, V, GF, amb, sinw

 B0(NF)=33.D0-2.D0*NF
 B1(NF)=6.D0*(153.D0-19.D0*NF)/B0(NF)**2
 B2(NF)=27/2.D0*(2857-5033/9.D0*NF+325/27.D0*NF**2)/B0(NF)**3
 B3(NF)= 81*(149753/6.d0+3564*zeta3-(1078361/162.d0+6508*zeta3/27)
     .          *nf+(50065/162.d0+6472*zeta3/81)*nf**2+1093/729.d0*nf**3)
     .       / B0(NF)**4
 ALS2(NF,X,XLB)=12.D0*PI/(B0(NF)*DLOG(X**2/XLB**2))
     .                *(1.D0-B1(NF)*DLOG(DLOG(X**2/XLB**2))
     .                /DLOG(X**2/XLB**2))
 ALS3(NF,X,XLB)=12.D0*PI/(B0(NF)*DLOG(X**2/XLB**2))
     .              *(1.D0-B1(NF)*DLOG(DLOG(X**2/XLB**2))
     .               /DLOG(X**2/XLB**2)
     .               +(B1(NF)**2*(DLOG(DLOG(X**2/XLB**2)))**2
```

```
       .                              -DLOG(DLOG(X**2/XLB**2))-1)+B2(NF))
       .                   /DLOG(X**2/XLB**2)**2)
 ALS4(NF,X,XLB)=12.D0*PI/(B0(NF)*DLOG(X**2/XLB**2))
       .                *(1.D0-B1(NF)*DLOG(DLOG(X**2/XLB**2))
       .                 /DLOG(X**2/XLB**2)
       .                 +(B1(NF)**2*(DLOG(DLOG(X**2/XLB**2)))**2
       .                              -DLOG(DLOG(X**2/XLB**2))-1)+B2(NF))
       .                 /DLOG(X**2/XLB**2)**2
       .                 -(B1(NF)**3*(DLOG(DLOG(X**2/XLB**2)))**3
       .                              -5*DLOG(DLOG(X**2/XLB**2))**2/2
       .                              -2*DLOG(DLOG(X**2/XLB**2))+1/2.d0)
       .                  +3*B1(NF)*B2(NF)*DLOG(DLOG(X**2/XLB**2))
       .                  -B3(NF)/2)/DLOG(X**2/XLB**2)**3)
 AA(NF)=12D0*PI/B0(NF)
 BB(NF)=B1(NF)/AA(NF)
 CC(NF)=B2(NF)/AA(NF)
 DD(NF)=B3(NF)/AA(NF)
 XIT(A,B,X)=A/2.D0*(1D0+DSQRT(1D0-4D0*B*DLOG(X)))
 XIT3(A,B,C,X)=A/2.D0*(1D0+DSQRT(1D0-4D0*B*DLOG(X)
       .              *(1-(A*B*(DLOG(X)**2-DLOG(X)-1)+C/B)/X/DLOG(X))))
 XIT4(A,B,C,D,X)=A/2.D0*(1D0+DSQRT(1D0-4D0*B*DLOG(X)
       .              *(1-(A*B*(DLOG(X)**2-DLOG(X)-1)+C/B)/X/DLOG(X)
       .              +(A**2*B**2*(DLOG(X)**3-5*DLOG(X)**2/2-2*DLOG(X)+1/2.D0)
       .               +3*A*C*DLOG(X)-D/B/2)/X**2/DLOG(X))))
 PI=4.D0*DATAN(1.D0)
 N3LO = 0
 ZETA2 = PI**2/6
 ZETA3 = 1.2020569031595942853997381D0
 NF=5
 Q=AMZ
 XLB=Q*DEXP(-AA(NF)/ALP/2.D0)
 IF(NO.EQ.1)GOTO 111
 II=0
1      II=II+1
 X=DLOG(Q**2/XLB**2)
 A=AA(NF)/ALP
 B=BB(NF)*ALP
 C=CC(NF)*ALP
 D=DD(NF)*ALP
 IF(NO.EQ.2)THEN
 XX=XIT(A,B,X)
 ELSEIF(NO.EQ.3)THEN
 XX=XIT3(A,B,C,X)
 ELSE
 XX=XIT4(A,B,C,D,X)
 ENDIF
 IF(N3LO.NE.0) XX=XIT4(A,B,C,D,X)
 XLB=Q*DEXP(-XX/2.D0)
 Y1=ALP
 IF(NO.EQ.2)THEN
```

```
 Y2=ALS2(NF,Q,XLB)
 ELSEIF(NO.EQ.3)THEN
 Y2=ALS3(NF,Q,XLB)
 ELSE
 Y2=ALS4(NF,Q,XLB)
 ENDIF
 IF(N3LO.NE.0) Y2=ALS4(NF,Q,XLB)
 DY=DABS(Y2-Y1)/Y1
 IF(DY.GE.ACC) GOTO 1
111   XITLA=XLB
 RETURN
 END


 SUBROUTINE pdfset(pathname,pdfname)
 IMPLICIT DOUBLE PRECISION (A-H,O-Z)
 character*30 pdfname, pathname
 common/pdflib/ngroup,nset,scalfac
 common/pdflib0/iseterr,ials
 if(ngroup.eq.0)then
 call SetPDFpath(pathname)
 call InitPDFsetByName(pdfname)
 call InitPDF(nset)
 endif
 RETURN
 END


 SUBROUTINE STRUC(X,Q,PDF)
 IMPLICIT DOUBLE PRECISION (A-H,O-Z)
 DIMENSION PDF(-6:6), VALUE(20)
 COMMON/PDFLIB/NGROUP,NSET,scalfac
 IPDFLIB=NGROUP
 CALL EVOLVEPDF(X,Q,PDF)
 PDF(6)=0
 PDF(-6)=0
 RETURN
 END
```

Now we show an example of soubroutine called from the integrand function to get the triangle contribution

```
      subroutine triangle(ampt1,g,gs,mt,s,g4h,s1,s2,g3h,mh,pi,mw)
      implicit none
#include "/Library/Mathematica/Applications/LoopTools-2.16/x86_64-Darwin/include/looptoc
      complex*16 ampt1
      double precision g,gs,mt,s,g4h,s1,s2,g3h,mh,pi,mw
      call ltini
  ampt1=0.0625D0*
     &(g*gs**2.D0*mt**2.D0*
     &(2.D0+C0(s,0.D0,0.D0,mt**2.D0,mt**2.D0,mt**2.D0)*
     &(4.D0*mt**2.D0-1.D0*s))*
     &(s*(g4h*s1*s2+g3h*(s1+s2))+2.D0*(g4h*mh**6.D0)-
```

```
    &mh**4.D0*(3.D0*g3h-g4h*(s-3.D0*(s1+s2)))-
    &1.D0*(g3h*s1**2.D0+(g3h*s1+g4h*s1**2.D0)*s2+
    &(g3h+g4h*s1)*s2**2.D0)+
    &mh**2.D0*(g4h*(s1**2.D0+s2**2.D0)+3.D0*(g3h*s1)+
    &s2*(3.D0*g3h+4.D0*(g4h*s1))-
    &1.D0*(s*(2.D0*g3h+1.D0*(g4h*(s1+s2)))))))/
    &(mw*pi**2*(mh**2.D0-1.D0*s)*(mh**2.D0-1.D0*s1)*
    &(mh**2.D0-1.D0*s2)*(2.D0*mh**2.D0+1.D0*s-1.D0*(s1+s2)))

  end subroutine triangle
```

# Bibliography

[1] **ATLAS** Collaboration, G. Aad et al., "Observation of a new particle in the search for the Standard Model Higgs boson with the ATLAS detector at the LHC," Phys. Lett. B **716** (2012) 1–29, arXiv:1207.7214 [hep-ex].

[2] **CMS** Collaboration, S. Chatrchyan et al., "Observation of a New Boson at a Mass of 125 GeV with the CMS Experiment at the LHC," Phys. Lett. B **716** (2012) 30–61, arXiv:1207.7235 [hep-ex].

[3] J. Goldstone, A. Salam, and S. Weinberg, "Broken symmetries," Physical Review **127** no. 3, (1962) 965.

[4] S. Weinberg, "A model of leptons," Physical review letters **19** no. 21, (1967) 1264.

[5] G. S. Guralnik, C. R. Hagen, and T. W. Kibble, "Global conservation laws and massless particles," Physical Review Letters **13** no. 20, (1964) 585.

[6] P. W. Higgs, "Broken symmetries, massless particles and gauge fields," Phys. Lett. **12** (1964) 132–133.

[7] J. F. Gunion, H. E. Haber, G. L. Kane, and S. Dawson, The Higgs Hunter's Guide, vol. 80 of Frontiers in Physics. Addison-Wesley, 1990.

[8] **CMS** Collaboration, A. M. Sirunyan et al., "Combined measurements of Higgs boson couplings in proton–proton collisions at $\sqrt{s} = 13\,\text{TeV}$," Eur. Phys. J. C **79** no. 5, (2019) 421, arXiv:1809.10733 [hep-ex].

[9] **ATLAS** Collaboration, G. Aad et al., "Study of the spin and parity of the Higgs boson in diboson decays with the ATLAS detector," Eur. Phys. J. C **75** no. 10, (2015) 476, arXiv:1506.05669 [hep-ex]. [Erratum: Eur.Phys.J.C 76, 152 (2016)].

[10] **ATLAS** Collaboration, G. Aad et al., "A detailed map of Higgs boson interactions by the ATLAS experiment ten years after the discovery," Nature **607** no. 7917, (2022) 52–59, arXiv:2207.00092 [hep-ex]. [Erratum: Nature 612, E24 (2022)].

[11] **CMS** Collaboration, A. Tumasyan et al., "A portrait of the Higgs boson by the CMS experiment ten years after the discovery.," Nature **607** no. 7917, (2022) 60–68, arXiv:2207.00043 [hep-ex]. [Erratum: Nature 623, (2023)].

[12] S. Borowka, N. Greiner, G. Heinrich, S. Jones, M. Kerner, J. Schlenk, U. Schubert, and T. Zirke, "Higgs boson pair production in gluon fusion at next-to-leading order with full top-quark mass dependence," Physical Review Letters **117** no. 1, (June, 2016) . http://dx.doi.org/10.1103/PhysRevLett.117.012001.

[13] M. Grazzini, G. Heinrich, S. Jones, S. Kallweit, M. Kerner, J. M. Lindert, and J. Mazzitelli, "Higgs boson pair production at nnlo with top quark mass effects," Journal

of High Energy Physics **2018** no. 5, (May, 2018) .
http://dx.doi.org/10.1007/JHEP05(2018)059.

[14] D. de Florian, I. Fabre, and J. Mazzitelli, "Triple higgs production at hadron colliders at nnlo in qcd," Journal of High Energy Physics **2020** no. 3, (2020) 1–24.

[15] R. Bonciani, G. Degrassi, P. P. Giardino, and R. Gröber, "Analytical method for next-to-leading-order qcd corrections to double-higgs production," Physical Review Letters **121** no. 16, (2018) 162003.

[16] L. Alasfar, G. Degrassi, P. P. Giardino, R. Gröber, and M. Vitti, "Virtual corrections to gg→ zh via a transverse momentum expansion," Journal of High Energy Physics **2021** no. 5, (2021) 1–19.

[17] G. Degrassi, R. Gröber, and M. Vitti, "Virtual qcd corrections to $gg \to zz$: top-quark loops from a transverse-momentum expansion," arXiv preprint arXiv:2404.15113 (2024) .

[18] "A detailed map of higgs boson interactions by the atlas experiment ten years after the discovery," Nature **607** no. 7917, (2022) 52–59.

[19] M. E. Peskin, An introduction to quantum field theory. CRC press, 2018.

[20] W. Marciano and H. Pagels, "Quantum chromodynamics," Physics Reports **36** no. 3, (1978) 137–276.

[21] S. D. Joglekar and B. W. Lee, "General theory of renormalization of gauge invariant operators," Annals of Physics **97** no. 1, (1976) 160–215.

[22] A. Djouadi, "The anatomy of electroweak symmetry breaking tome ii: The higgs bosons in the minimal supersymmetric model," Physics reports **459** no. 1-6, (2008) 1–241.

[23] D. J. Gross and F. Wilczek, "Ultraviolet behavior of non-abelian gauge theories," Physical Review Letters **30** no. 26, (1973) 1343.

[24] J. C. Collins, D. E. Soper, and G. Sterman, "Factorization of hard processes in qcd," arXiv preprint hep-ph/0409313 (2004) .

[25] A. Buckley, J. Ferrando, S. Lloyd, K. Nordström, B. Page, M. Rüfenacht, M. Schönherr, and G. Watt, "Lhapdf6: parton density access in the lhc precision era," The European Physical Journal C **75** (2015) 1–20.

[26] **NNPDF** Collaboration, R. D. Ball et al., "The path to proton structure at 1% accuracy," Eur. Phys. J. C **82** no. 5, (2022) 428, arXiv:2109.02653 [hep-ph].

[27] E. Byckling and P. Pirilä, "Invariant and angular variables for five particle processes," Zeitschrift für Physik A Hadrons and nuclei **250** no. 5, (1972) 379–386.

[28] E. Byckling and K. Kajantie, "Particle kinematics,".

[29] G. P. Lepage, "A new algorithm for adaptive multidimensional integration," Journal of Computational Physics **27** no. 2, (1978) 192–203.

[30] T. Hahn, "Cuba—a library for multidimensional numerical integration," Computer Physics Communications **168** no. 2, (2005) 78–95.

[31] R. Kleiss, S. Ellis, and W. J. Stirling, "A new monte carlo treatment of multiparticle phase space at high energies," Comput. Phys. Commun. **40** no. CERN-TH-4299-85, (1985) 359–373.

[32] T. Hahn, "Generating feynman diagrams and amplitudes with feynarts 3," Computer Physics Communications **140** no. 3, (2001) 418–431.

[33] M. Spira, "Higgs boson production and decay at hadron colliders," Progress in Particle and Nuclear Physics **95** (2017) 98–159.

[34] T. Plehn, M. Spira, and P. Zerwas, "Pair production of neutral higgs particles in gluon-gluon collisions," Nuclear Physics B **479** no. 1-2, (1996) 46–64.

[35] E. N. Glover and J. J. Van der Bij, "Higgs boson pair production via gluon fusion," Nuclear Physics B **309** no. 2, (1988) 282–294.

[36] R. Mertig, M. Böhm, and A. Denner, "Feyn calc-computer-algebraic calculation of feynman amplitudes," Computer Physics Communications **64** no. 3, (1991) 345–359.

[37] V. Shtabovenko, R. Mertig, and F. Orellana, "New developments in feyncalc 9.0," Computer Physics Communications **207** (2016) 432–444.

[38] V. Shtabovenko, R. Mertig, and F. Orellana, "Feyncalc 9.3: New features and improvements," Computer Physics Communications **256** (2020) 107478.

[39] M. D. Schwartz, Quantum field theory and the standard model. Cambridge university press, 2014.

[40] M. Veltman and G. 't Hooft, "Scalar one-loop integrals," Nuclear Physics B **153** (1979) 365–401.

[41] J. C. Romao, "Modern techniques for one-loop calculations," Version **1** (2004) 263.

[42] G. Van Oldenborgh and J. A. Vermaseren, "New algorithms for one-loop integrals," Zeitschrift für Physik C Particles and Fields **46** (1990) 425–437.

[43] T. Hahn and M. Perez-Victoria, "Automated one-loop calculations in four and d dimensions," Computer Physics Communications **118** no. 2-3, (1999) 153–165.

[44] A. Denner and S. Dittmaier, "Reduction of one-loop tensor 5-point integrals," Nuclear Physics B **658** no. 1-2, (2003) 175–202.

[45] T. Hahn, "Automatic loop calculations with feynarts, formcalc, and looptools," Nuclear Physics B-Proceedings Supplements **89** no. 1-3, (2000) 231–236.

[46] J. Davies, G. Mishima, K. Schönwald, and M. Steinhauser, "Analytic approximations of $2 \rightarrow 2$ processes with massive internal particles," Journal of High Energy Physics **2023** no. 6, (2023) 1–26.

[47] Laporta International Journal of Modern Physics A **15** (2000) 5087. http://dx.doi.org/10.1016/S0217-751X(00)00215-7.

[48] R. N. Lee, "Presenting litered: a tool for the loop integrals reduction," 2012. https://arxiv.org/abs/1212.2685.

[49] R. N. Lee, "Litered 1.4: a powerful tool for reduction of multiloop integrals," Journal of Physics: Conference Series **523** (June, 2014) 012059. http://dx.doi.org/10.1088/1742-6596/523/1/012059.

[50] V. A. Smirnov, Analytic tools for Feynman integrals. Springer, 2013.